CHAPTER 5

INTERPRETATION AND DISCUSSION OF GEOCHEMISTRY, GEOCHRONOLOGY, AND TECTONICS OF THE EYJAFJÖLL VOLCANIC SYSTEM

Geochemistry

Mineral Data - Magma Dynamics

Study of mineral compositions, mineral textures and structures in thin section, as described in detail in the last chapter, suggests that mixing of phenocrysts and their host magmas plays a major role in the genesis of Eyjafjöll rocks. Nearly all phenocrysts show disequilibrium textures and microprobe analysis shows that there are multiple populations and compositions within single samples. It is inferred that the phenocrysts present in these rocks are derived from multiple magmas (or crystal mushes). This idea is corroborated by the work of Meyer et al. (1985), which used petrographic data from Hekla and Katla to suggest that mixing of magmas of extreme compositions (such as Fe-Ti basalts and tholeiites) occurs for these systems in particular, and perhaps for the SEVZ as a whole. A mechanism must exist, then, which would allow for the magmas carrying phenocrysts to change composition or for the phenocrysts to separate from the magmas with which they are in equilibrium, and accumulate in others.

Magma mixing is one possible mechanism for creating multiple phenocryst populations. When magmas of two different compositions mix, the resulting new composition will leave the already formed phenocrysts in disequilibrium. During reequilibration, zoning can result as follows. Reversed zoning will occur for the phenocrysts from the more evolved magma of the original two, as a more primitive rim crystallizes around an evolved

core. Normal zoning will result for the phenocrysts of the more primitive magma of the original two as an evolved rim forms around a primitive core. Finally, new phenocrysts formed in equilibrium with the new magma composition will show little to no zoning. (This is, of course, a simplified description. If changes in composition are high enough, the more evolved phenocrysts could melt rather than grow rims). A direct result of this scenario is existence within one melt of phenocrysts with three different core compositions. The olivines from sample Ey-17 show this very well (Figure 5.01), where three different core compositions and corresponding zoning types are found. (Normal zoning for the most primitive olivine cores, reversed for the most evolved olivine cores, and no zoning for the intermediary composition.) It is important to note from this figure that the core compositions are different, but not dramatically so. If mixing is used to explain this, then the compositional differences in magmas need not be large. Perhaps even mixing of different zones within a magma chamber would be enough.

For magma mixing to be the mechanism responsible for the observed textures and zoning, the olivines must be maintained, suspended within the melt; they cannot separate (gravitationally settle). As olivine is denser than any of the observed melt compositions, the only ways for settling not to occur are for the crystals to be too small, for the viscosity of the magma to be too large to allow the settling, for mixing and eruption to occur before the crystals have had time to separate, or for the crystals to be dynamically entrained in the melt.

Another mechanism which can explain the observed multiple phenocryst compositions is separation of the crystals from the melt and accumulation in distinct zones where they can later be incorporated into different magmas. If

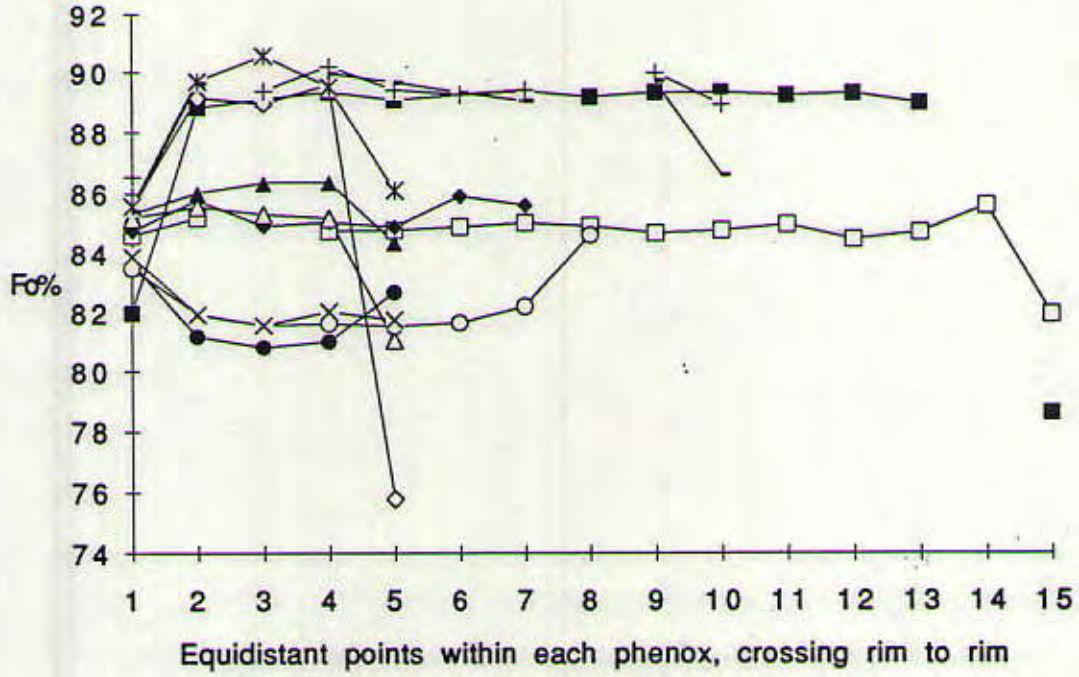

Figure 5.01: Representative olivine phenocrysts from Ey-17, showing three different core compositions. Data are from microprobe transects of individual crystals from rim to rim. Phenocrysts with more points usually indicate larger phenocrysts. Missing data signifies an error (usually hitting an inclusion) during microprobe analysis.

there were a zone under Eyjafjöll where melts could reside and undergo crystal fractionation, it would be possible for the minerals to separate. The conditions under which this would be possible are dependent upon crystal and magma density, magma viscosity, crystal size and residence time. Olivine and other high density minerals will sink, while plagioclase will float to the top of the magma. As crystallization continues, the magmas will become more evolved, as will the crystallizing minerals. A zone of cumulate material can develop which will be filled with minerals spanning a large range of compositions. If a new magma is injected, either mixing with the older, now more evolved magma, or pushing the older magma upwards for eruption, the cumulate zones can change as follows. (A) Crystals from the zones can become entrained into the erupting magma and thus be out of equilibrium upon eruption. (B) Crystals from the zones can be partially reincorporated into the new magma and attempt equilibration before returning (sink/float) to their accumulation zones. These crystals will show multiple disequilibrium textures. (C) Crystals from the zones can remain untouched, but crystals from the new magma can be added. The plagioclase compositions from the Eyjafjöll samples suggest that all of these types of mechanisms are occurring. This is best seen in sample Ey-10 (Figure 5.02), where multiple core compositions exist for plagioclase crystals and all types of zoning occur: normal, reversed (entrainment of crystal into more primitive magma), and oscillatory (multiple episodes of reequilibration.)

Microprobe data from the Eyjafjöll system, as shown in detail in Appendix D, suggest that both of these mechanisms, magma mixing (on a small scale), and crystal separation with later entrainment, are important in the genesis of the rocks from this system. The former mechanism, magma mixing, is best evidenced by olivine, while the latter mechanism, crystal separation,

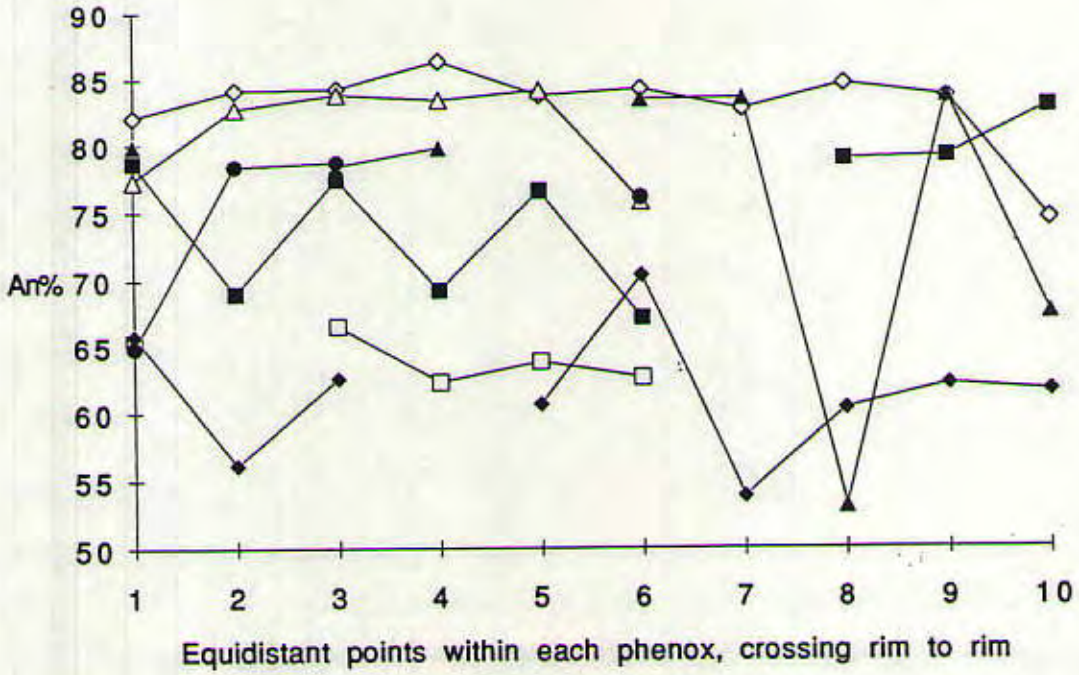

Figure 5.02: Representative plagioclase phenocrysts from Ey-10, showing multiple core compositions and zoning types. Data are from microprobe transects of individual crystals from rim to rim. Phenocrysts with more points usually indicate larger phenocrysts. Missing data signifies an error (usually hitting an inclusion) during microprobe analysis.

by plagioclase. Textural evidence, as discussed in the last chapter, supports plagioclase separation, as these crystals show abundant disequilibrium textures, and varied zoning geometries. Similarly, the microprobe data frequently show oscillatory zoning with major changes in composition. Olivine, on the other hand, shows very little disequilibrium texture, dominantly occurring as euhedral, clean phenocrysts. Microprobe data of these olivine crystals, however, consistently show minor and gradual zoning. The olivines appear to remain with the magmas (suspended dynamically), while the plagioclase crystals float to the top and accumulate. This will be discussed further below.

Chemical Data - Crystallization Models

Major and trace element data are plotted in variation diagrams (Figure 5.03, a-m) together with models used to determine the genetic relationship among samples. The program MIXNFRAC (Nielsen, 1990) was run to model simple closed-system fractional crystallization with no recharge, assimilation or eruption (0-0-0). This model was run for a starting magma composition at 1 atm pressure, under anhydrous conditions and therefore represents only a comparison model, as the material from Eyjafjöll was most likely crystallizing in the presence of water and at moderate pressures. The program includes distribution coefficients for the crystallizing assemblages which are drawn from experimental data. Phase assemblages are determined by a combination of mass balance and thermodynamic equations, the former determined by starting composition, the latter by experimental data, and oxygen fugacity (Nielsen, 1990). The liquid compositions derived from this model are shown alongside the Eyjafjöll data in all of the oxide variation diagrams.

Each model begins with a parent composition, for which Ey-49 was chosen. An ideal parent composition would be one with no phenocrysts and

Figure 5.03 (a-m): Major (a-h) and trace (i-m) element variation diagrams, including data for the Eyjafjöll Volcanic System, and trends for perfect fractional crystallization models (MIXNFRAC) at the NNO buffer and QFM buffer. Cumulates indicate the four samples referred to in the text as ankaramites and picrites. Arrows represent addition of phenocrysts and are labelled accordingly.

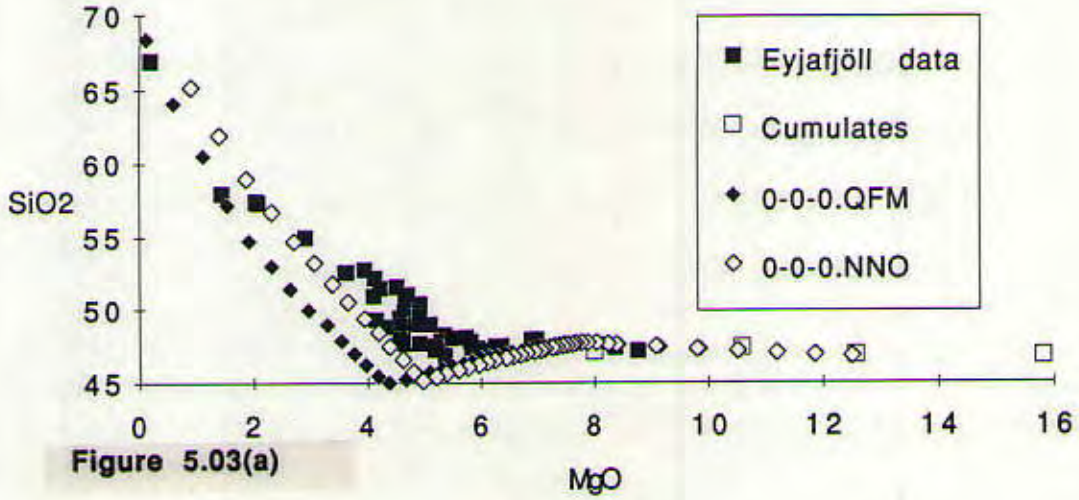

Figure 5.03(a)

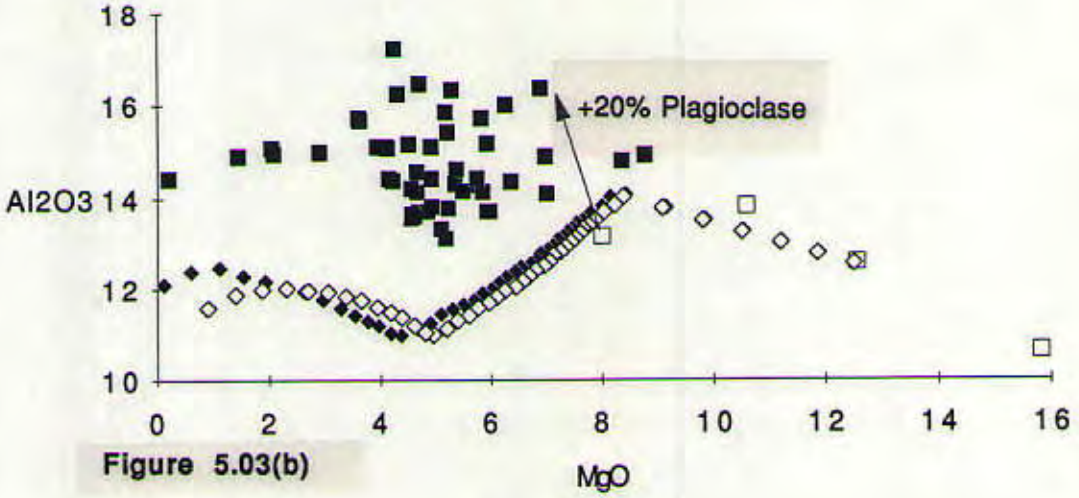

Figure 5.03(b)

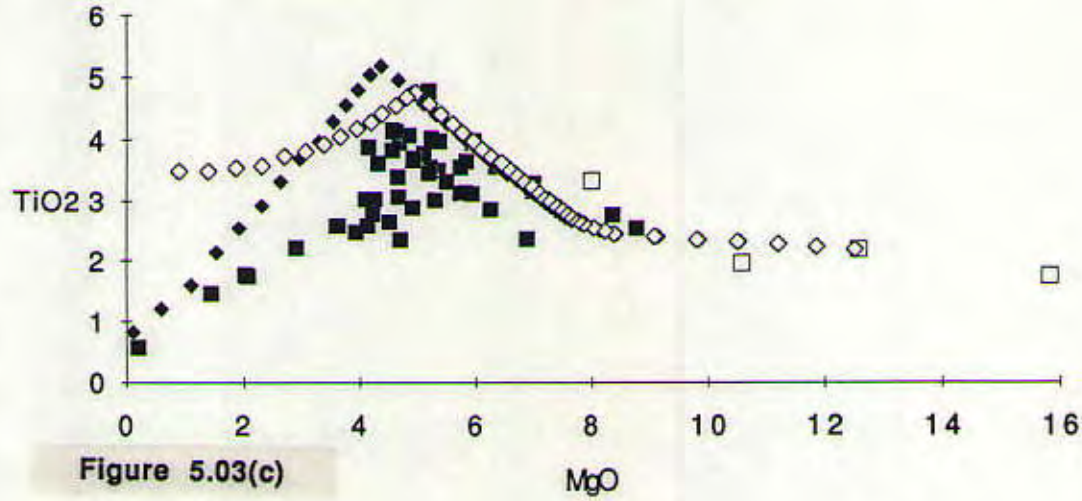

Figure 5.03(c)

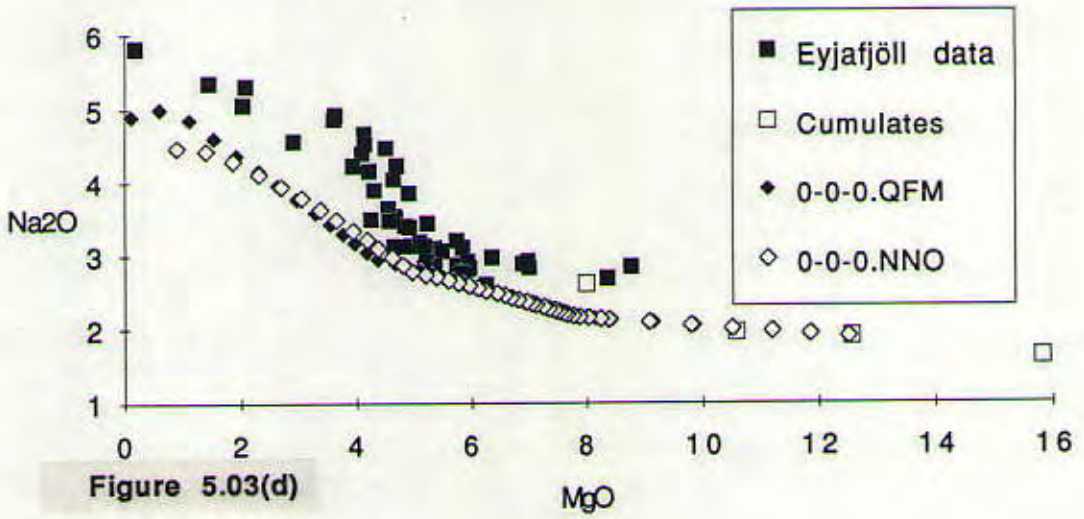

Figure 5.03(d)

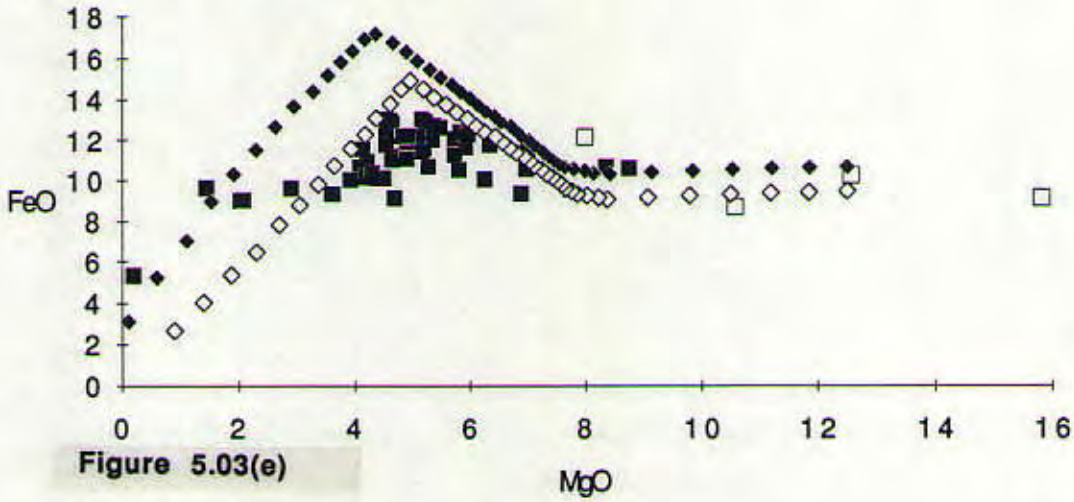

Figure 5.03(e)

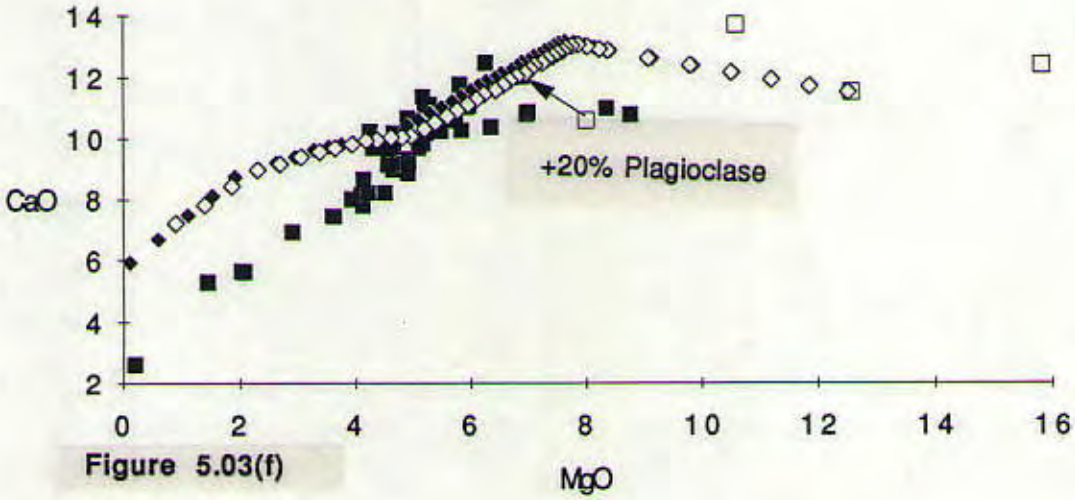

Figure 5.03(f)

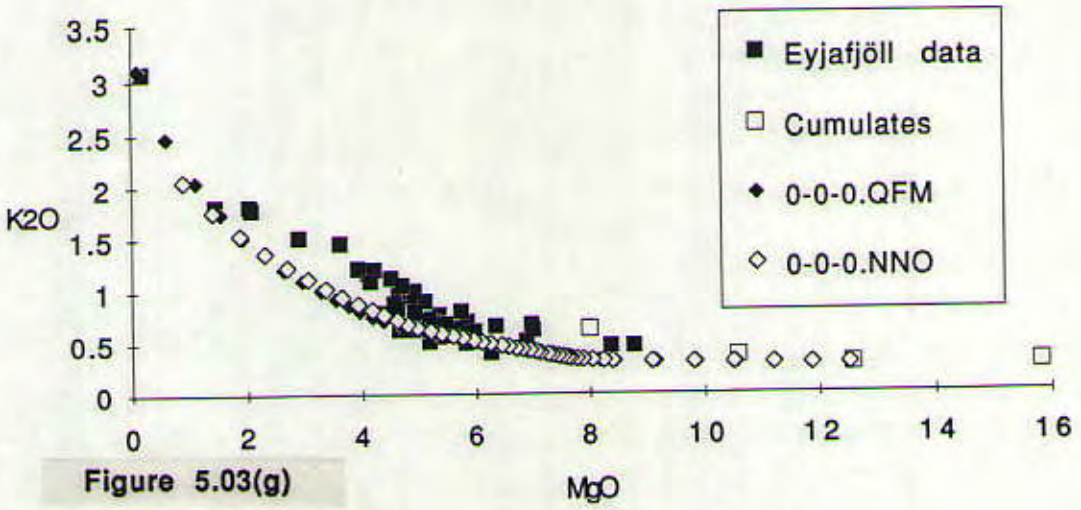

Figure 5.03(g)

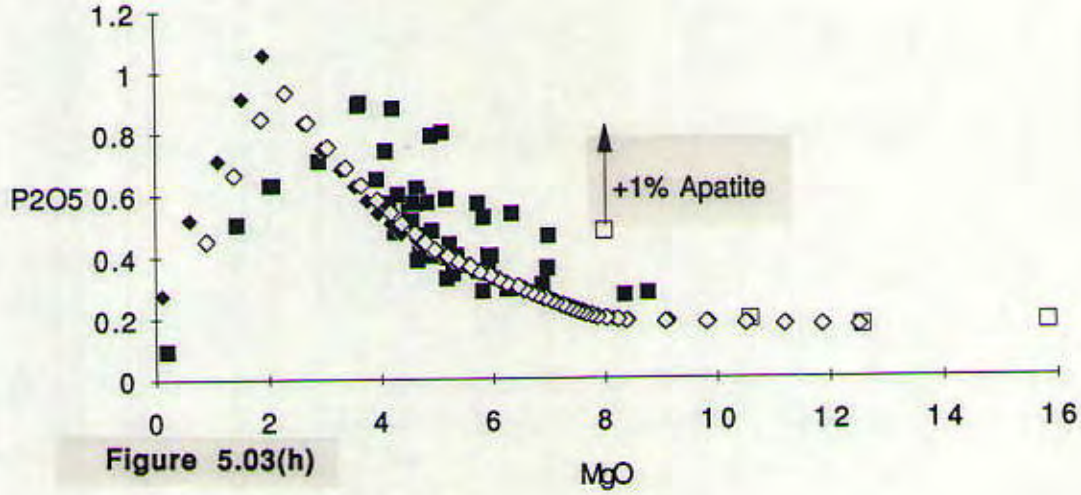

Figure 5.03(h)

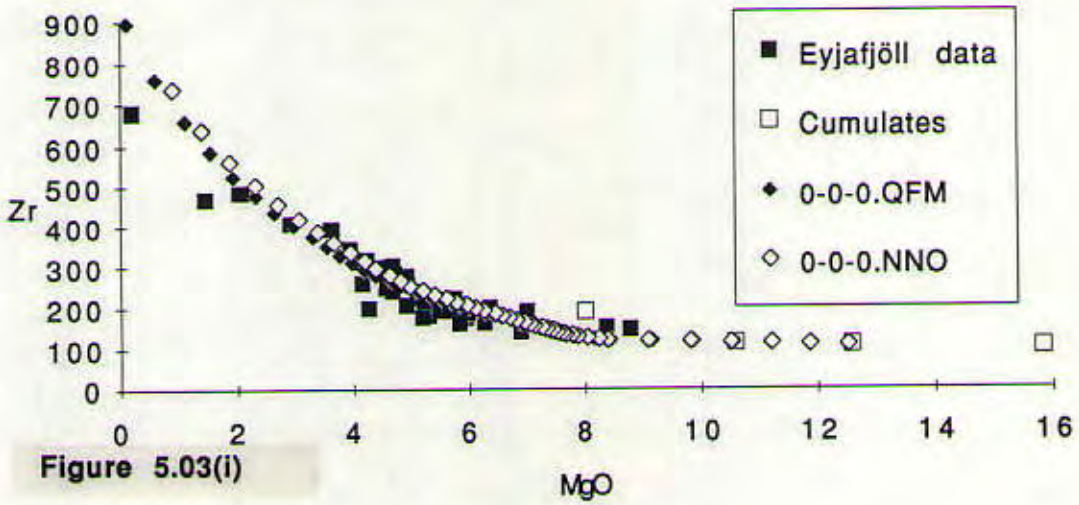

Figure 5.03(i)

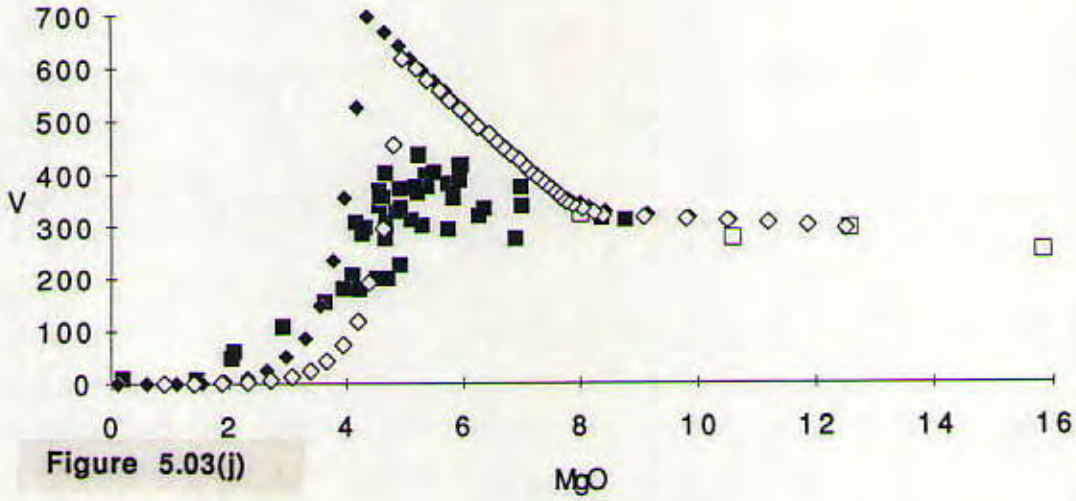

Figure 5.03(j)

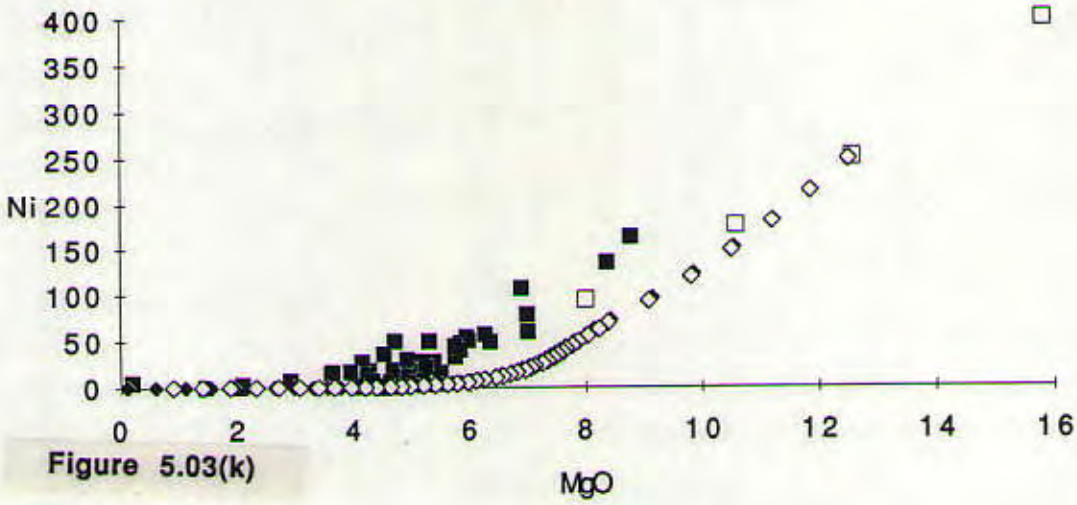

Figure 5.03(k)

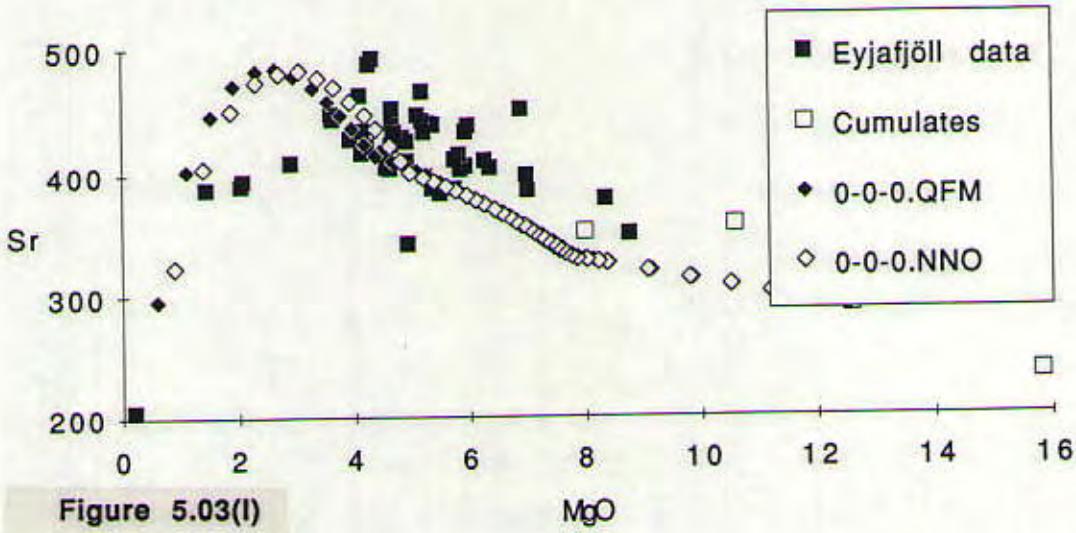

Figure 5.03(l)

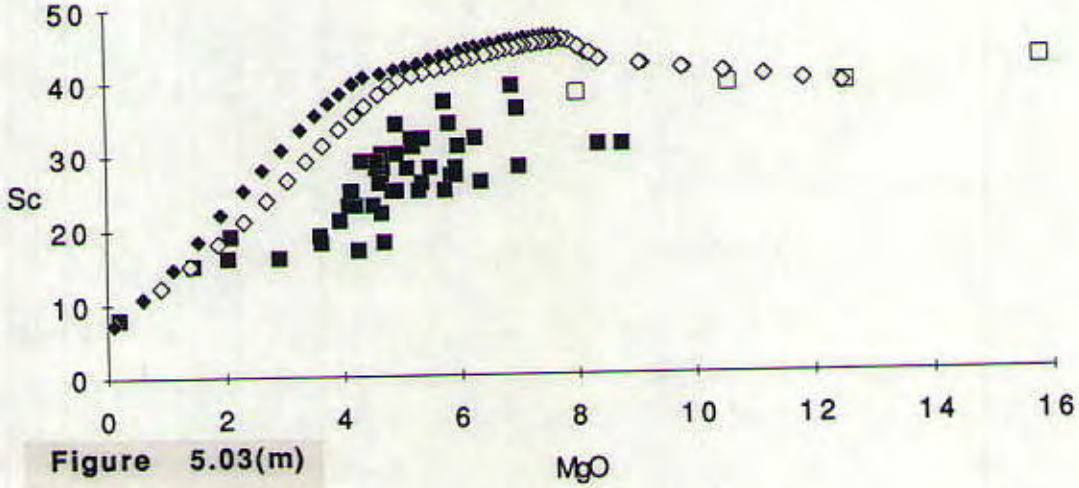

Figure 5.03(m)

representing a composition just above the liquidus for plagioclase (with only olivine fractionation having occurred). After observing the trends present in the real data and comparing these with modeled predictions, a hypothetical parent composition was created according to the above criteria. The MIXNFRAC (0-0-0) model was then run backwards (addition of olivine) from this composition and found to form a composition similar to that of Ey-49 (a cumulate rock with mostly olivine phenocrysts). Ey-49 was used as the parent composition in all subsequent models. The MIXNFRAC (0-0-0) model is shown in all plots for the nickel-nickel oxide (NNO) and quartz-fayalite-magnetite (QFM) oxygen fugacity buffers. What is most important to note in the diagrams is that in form the modeled liquids seem quite similar to the real data. The instances where the model is different from the real data can be explained by differences in the conditions under which the model was run, such as higher pressures and presence of water. These are discussed below.

At first glance, the Eyjafjöll data seem to lie along or within most of the modeled trends. Most of the scatter can be explained by mixing of evolved magmas with more primitive ones from along the simple fractional crystallization trend, in combination with varying amounts of phenocryst addition. Table 5.01 shows this quantitatively, where Ey-20 and Ey-28 (rocks with little to no phenocrysts which lie along the projected 0-0-0 trend) are mixed in the ratio of 1.5 to 1, and then accumulate 15% plagioclase (An80), 5% cpx (average phenocryst composition) and 2% titanomagnetite in an attempt to generate Ey-11 (a rock with 20% phenocrysts, plag>cpx>oxides). The resulting composition is shown in comparison to Ey-11 and a fractional error is given as well. For this particular example, the calculations fit well. Another example given is for 10% plagioclase

Table 5.01: Chemical effects of magma mixing and crystal accumulation.

MIXING TWO MAGMAS	Ey-20	Ey-28	Mix ratio 1.5 to 1	add15% plag	add 5% cpx	add 2% timag	Sample with 20% phenocrysts Ey-11	fractional error
SiO2	47.41	50.89	48.80	48.68	48.70	47.74	47.79	1.00
Al2O3	14.10	15.09	14.50	17.01	16.48	16.19	16.30	1.01
TiO2	3.28	3.02	3.18	2.76	2.68	3.05	3.01	0.99
FeO	13.23	12.22	12.83	11.24	11.01	12.00	12.26	1.02
MnO	0.21	0.22	0.22	0.19	0.18	0.19	0.19	0.99
CaO	10.86	8.17	9.78	10.69	11.21	10.99	11.12	1.01
MgO	7.00	4.10	5.84	5.08	5.56	5.49	5.29	0.96
K2O	0.62	1.17	0.84	0.74	0.70	0.69	0.61	0.89
Na2O	2.83	4.39	3.45	3.29	3.14	3.08	3.09	1.00
P2O5	0.47	0.74	0.58	0.50	0.48	0.47	0.34	0.74
Totals	100.01	100.01	100.01	100.17	100.13	99.88	100.00	

PLAGIOCLASE ACCUMULATION	Ey-20	Ey-20 +10% An80	Ey-15	fractional error
SiO2	47.41	47.45	47.42	1.00
Al2O3	14.10	15.89	15.98	1.01
TiO2	3.28	2.98	2.85	0.96
FeO	13.23	12.09	11.54	0.95
MnO	0.21	0.19	0.18	0.92
CaO	10.86	11.39	12.47	1.09
MgO	7.00	6.37	6.26	0.98
K2O	0.62	0.57	0.40	0.70
Na2O	2.83	2.77	2.60	0.94
P2O5	0.47	0.42	0.29	0.70
Totals	100.01	100.12	99.99	

accumulation to explain the differences in composition between Ey-20 (no phenocrysts) and Ey-15 (10% plagioclase phenocrysts). Again the fit is good.

Some of the scatter in the TiO_2 plot can be explained by titanomagnetite accumulation, i.e. sample, Ey-1 (which plots at 8.00 wt.% MgO) has higher TiO_2 content than to the model. This rock is a cumulate and contains a relatively large number of titanomagnetite phenocrysts. These phenocrysts will elevate the amount of TiO_2 in the sample above that for perfect fractional crystallization, and yet won't affect any of the other element abundances except FeO which shows the same increase. This can be seen on both the TiO2 and FeO diagrams. The P_2O_5 plot shows mostly higher values for the real data than for the modeled predictions. This could indicate higher amounts of apatite in the rocks than the model suggests (or just an accumulation of apatite, instead of the removal inherent in the definition of fractional crystallization). Another explanation could be that the estimates of P_2O_5 for parent magmas are slightly less than they should be. However, careful study of the plot shows that the modeled locus of liquid compositions runs right along the bottom of the real data, and scatter lies just above this trend (higher in P_2O_5). This seems indicative of addition of crystals.

Some of the scatter on the Al_2O_3 plot is indicative of plagioclase accumulation. An arrow on this plot indicates addition of 20% plagioclase. This same arrow is shown for the CaO plot as well. No other elements would show detectable changes from this addition. (Plagioclase accumulation is also evident from the petrography which shows the dominance of plagioclase as a phenocryst in nearly every sample). Even with plagioclase addition, however, there are still major differences between the real data and the modeled data on both the CaO and Al_2O_3 plots. This will be discussed further below.

In order for plagioclase to float in the magmas it must maintain a lower density than the surrounding material and fulfill the other parameters necessary for Stoke's Law:

$$v = 2*g*r^2*(\rho(xl)-\rho(m))/(9*\eta)$$

where: v = settling velocity, g = gravity, r = crystal radius,

$\rho(xl)$ = crystal density, $\rho(m)$ = magma density, η = magma viscosity.

The densities of plagioclase and the surrounding melt, as both change composition during crystallization, are shown in Figure 5.04 for varying water content. It seems possible from these data alone that plagioclase will float in the Eyjafjöll melts as long as the water content of the starting material is not much more than 2%, and crystallization ceases around 1100 °C (70% crystallization). Any melts which proceed past this point will not be dense enough to allow plagioclase to float. The water content of the Eyjafjöll samples is unknown, but the vesicularity of many of the samples suggests that volatiles do play a role in at least the eruptive mechanics. For the system of Vestmannæyar just to the south, volatile contents are 0.30 wt% (loss on ignition analyses) for primitive (46.6 wt% SiO_2) basalts (Thy, 1991a). To the north, in Hekla, water content is estimated to be between 2.5 to 6 wt% depending upon how differentiated the material is (as discussed in Chapter 2, Baldridge et al., 1973). If this is a trend, as Meyer et al. (1985) suggest, with water content increasing northwards along the SEVZ, then Eyjafjöll should lie between these two endmembers, and thus be in a permissible zone for plagioclase accumulation. This is further supported by previous work suggesting that plagioclase accumulation is quite common throughout Iceland (Meyer et al., 1985).

Presence of water during crystallization for the Eyjafjöll system is different from the conditions under which the 0-0-0 models were run, and

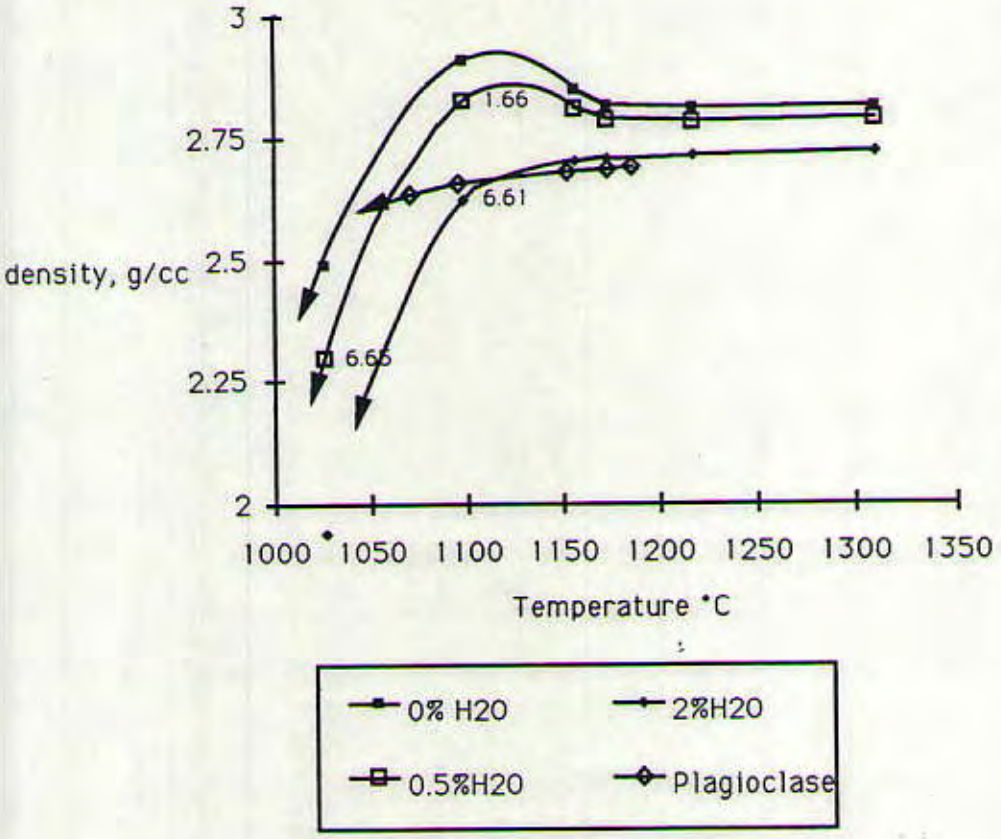

Figure 5.04: Change in density during crystallization of parent magma (Ey-49) at the NNO buffer. H_2O values given in the legend are for initial parent magma compositions. Numbers by data points are for H_2O values as crystallization continues. P = 3 Kbar; V(H_2O) = 17 cc/mole.

therefore can explain the difference between the real data and the modeled data for the Al_2O_3 diagrams. This is because, with addition of water, the liquidus temperature for plagioclase decreases, and therefore it enters the crystallization sequence later than anhydrous models predict (Hess, 1989). This can help explain the CaO plot as well, though not entirely. Again there appears to be a difference between the conditions under which the models were run and the real conditions of the system. The model was run a 1 atm, whereas evidence from the surrounding volcanic systems within the SEVZ suggests much higher pressures of crystallization. Hekla, to the north, has evidence of crystallization at 3-5 kbar, whereas Vestmannæyar, to the south shows 5-8 kbar crystallization. Most likely Eyjafjöll is somewhere in between (3-8 Kbar). A higher pressure would affect the crystallization sequence by having clinopyroxene enter earlier (Presnall et al., 1978; Stolper, 1980; Thy, 1991a, 1991b). As pressure increases, clinopyroxene becomes the first phase to crystallize. In the modeled trend clinopyroxene enters the sequence at about 20% crystallization. But the data suggest entrance earlier than that, most likely indicating increased pressures (higher than 1 atm) for the crystallization of these magmas. (Further evidence for this will be discussed in a later section).

Oxygen Fugacity, Crystallization Sequence, and Pressure

MIXNFRAC was run at both the NNO and QFM buffers, but it is the former that produces the best match to the data, in particular regarding the point at which oxides enter the crystallization sequence (if it is assumed that fractional crystallization is the dominant process occurring to the magmas of Eyjafjöll). In order to come up with another independent method of determining oxygen fugaciy, oxides from Ey-1 were analyzed by microprobe and these compositions were used in OXCALC (version 1.2 (1991): J.C. Stormer, Rice University), a

program which uses thermodynamic relationships to determine oxygen fugacity and corresponding crystallization/equilibration temperatures. The values derived from this program range from QFM to NNO and from 500°C to 1100°C. Only the highest temperature data are good representatives of the magmatic conditions, as the lower temperature values represent later, subsolidus equilibration reactions. The high temperature data, from Ey-1, lie along the NNO buffer (Table 4.03). This buffer has never been associated with oceanic basalts before and therefore necessitates further analysis to determine if this is real. Unfortunately this conclusion wasn't pursued any further during this project. However, oxygen fugacities determined for basalts from Vestmannæyar are found just above the QFM buffer (Thy, 1991b). Within sample Ey-1 there are a number of titanomagnetite phenocrysts, which all show exsolution (shown in Figure 4.18). In order to use the OXCALC program, separate compositions were needed for magnetite and ilmenite. When probing these phases, ilmenites were easy to find, having exsolved to form large regions within the crystals. Magnetite, however, if present as a distinct phase, was very small and hard to locate. The composition for the magnetite probed for the NNO value of Ey-1 comes from wide beam analyses (bulk) across the fine lamellae which surround the ilmenite sections. One sample phenocryst was also studied from Ey-4B but it shows equilibration temperatures lower than magmatic values, and isn't representative of the oxygen fugacity conditions of the volcanic system.

Further support for Eyjafjöll data following the NNO buffer comes from the correlation of the real data with the models on the oxide variation plots. The entrance of different phases (especially titanomagnetite) into the crystallization sequence is sensitive to oxygen fugacity, and the whole rock data (XRF data) agree best with the NNO models. For the NNO buffer, during the

evolution of the parent material, Ey-49, (at 1 atm with no water) the first mineral to crystallize is olivine (Fo89), at 1311°C. Mg-rich chromite begins to crystallize, along with olivine at 1254°C (6.1% crystallization). At 1187°C (12.2% crystallization) plagioclase (An77) begins to crystallize. At 1173°C (18.2% crystallization) spinel stops crystallizing, and only olivine and plagioclase remain, crystallizing in the ratio 1:2. Clinopyroxene enters the sequence at 1171°C (20.2% crystallization) when olivine is Fo84.1 and plagioclase is An75.4. Magnetite enters at 1165°C (62.2% crystallization) and at 1109°C (64.2% crystallization) olivine drops out. Apatite enters at 1081°C (84.5% crystallization). As mentioned earlier, higher pressures will increase the liquidus temperature of clinopyroxene until it becomes the first phase to crystallize. Addition of water will decrease the liquidus temperatures of all phases, most especially plagioclase.

What is particularly interesting regarding the modeled crystallization sequence, is the difference between NNO and QFM models. Again, the petrography supports NNO better than QFM. Major differences are that the QFM, 0-0-0 model shows no early spinel crystallization. Magnetite comes in later, at 1100°C and very late stage (>86.5% crystallization) pigeonite and orthopyroxene are present. The petrography shows no pigeonite or orthopyroxene, and does show early spinel crystallization (inclusions in olivine, clinopyroxene, and plagioclase). But even more noticeable is the point at which oxides enter the crystallization sequence (at later stages of fractionation), which corresponds quite well with NNO models, but not with the QFM models.

The petrography also provides further support for high pressure crystallization during which clinopyroxene enters the sequence earlier, and hydrous crystallization during which plagioclase enters later than 1 atm,

anhydrous models. This comes from clinopyroxene inclusions in plagioclase. There are rare plagioclase inclusions in olivine which can be explained by one of the following mechanisms: entrainment of crystals within a simultaneously crystallizing phase; or entrapment of a previously formed crystal into a primitive melt during crystallization (crystals coming from accumulation zones). Also under favorable conditions (low water contents) high-pressure crystallization will cause plagioclase to precede olivine for a very small increment. Which mechanism is actually occurring in these rocks can be determined by probing the inclusions to find out their compositions and comparing these with the modeled predictions. (This was not done in this study due to the scarcity of these inclusions and the consequent difficulty of finding them in probe sections.)

The titanium concentrations relative to the aluminum concentrations in clinopyroxene have been determined for varying crystallizing pressures (Figure 5.05, Thy, 1991a) for the Vestmannæyar system, and are found to change considerably. These relationships are calculated for the Eyjafjöll rocks and shown in Figures 5.06 and 5.07. It can be seen from these plots that the clinopyroxenes from Eyjafjöll represent crystallization in a large range of pressures from 1 atm to possibly as high as 10 Kbar. Because the crust under this region is so thick, these higher pressures seem quite reasonable.

Magma Chambers

There appears to be no difference in composition or structure among different geographical sampling sections within the Eyjafjöll Volcanic System. This is partly due to the fact that sections are all radially distributed, combining central and flank volcanism. The lack of a geographical pattern suggests that the source for all Eyjafjöll material is deep-seated and doesn't change for different eruptive centers on the volcano. The only exception to this

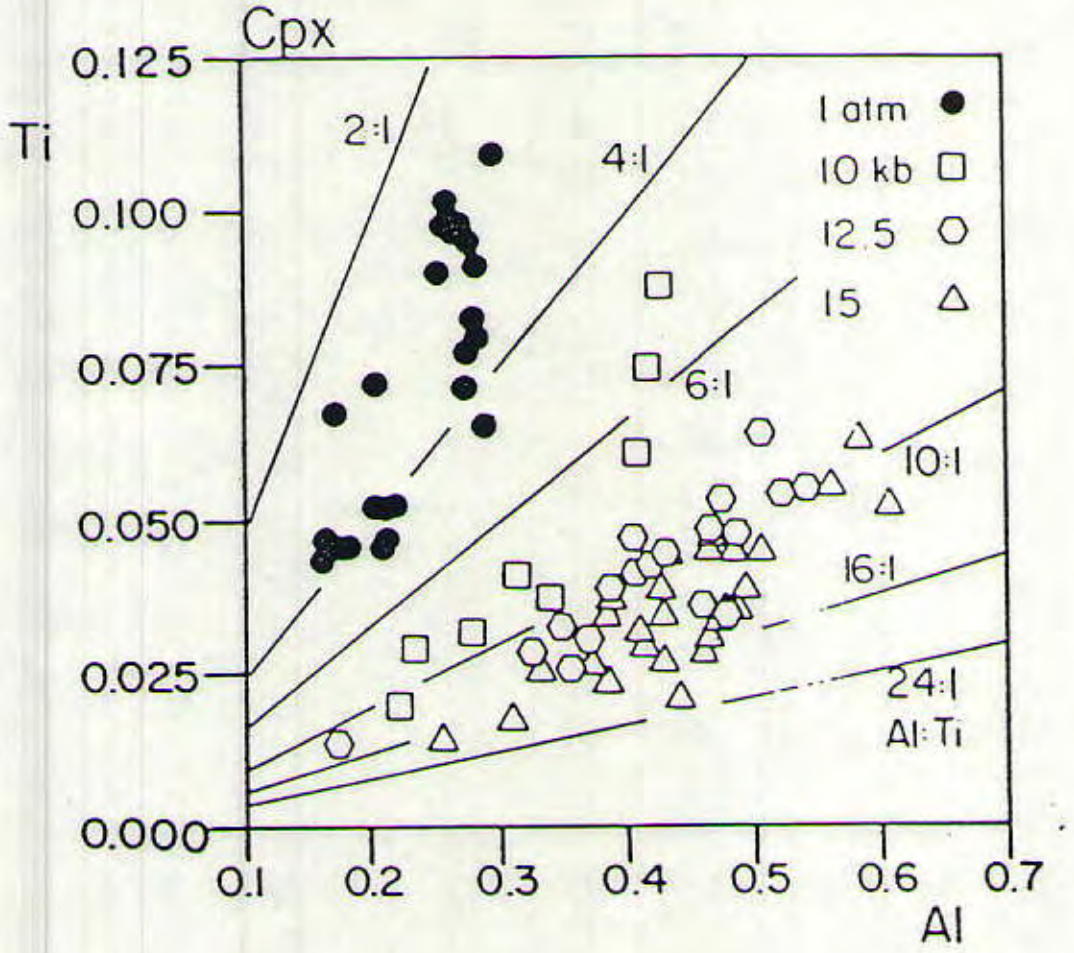

Figure 5.05: Ti vs. Al (cation mole fraction) for experimental clinopyroxenes from Vestmannæyar study (Thy, 1991a).

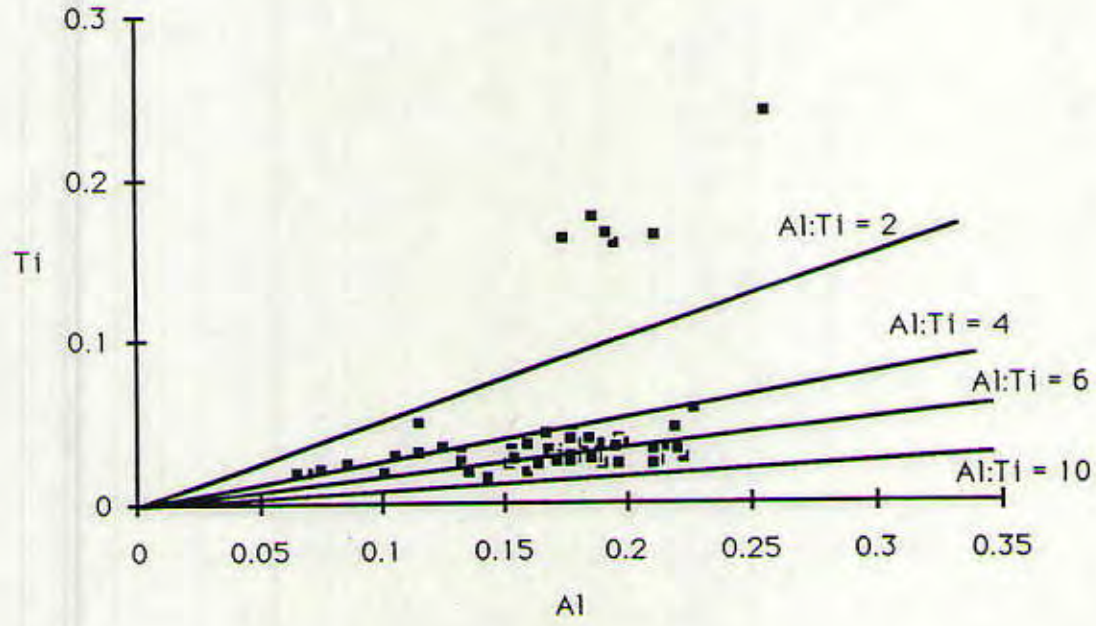

Figure 5.06: Ti vs. Al (cation mole fraction) for clinopyroxenes from Eyjafjöll data (full range of Ti data).

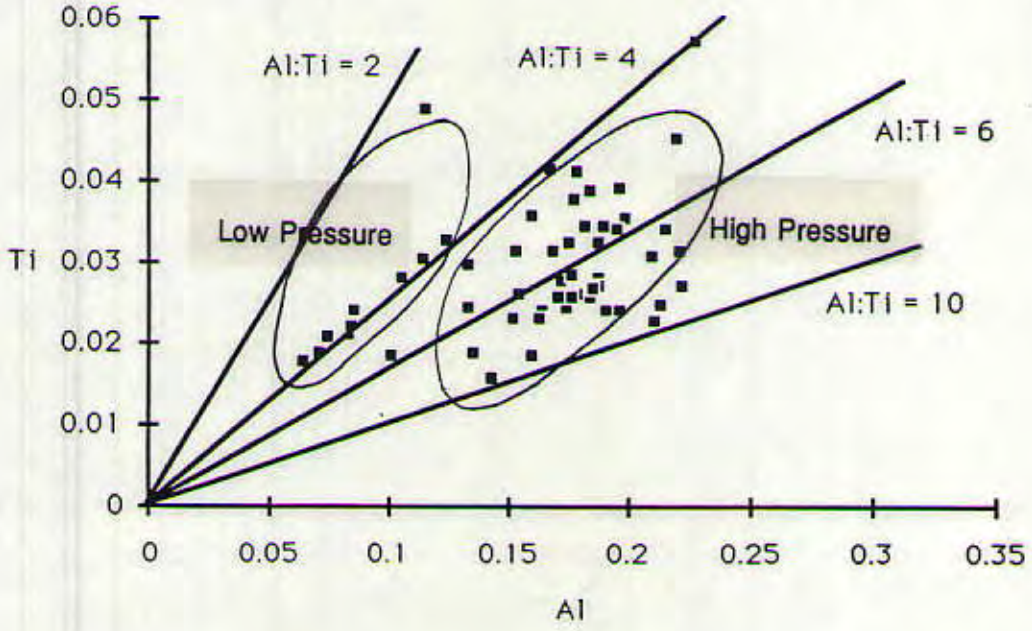

Figure 5.07: Ti vs. Al (cation mole fraction) for clinopyroxenes from Eyjafjöll data (limited range of Ti data).

is that all of the most fractionated samples come from the central portions of the complex. This is indicative (as with Hekla to the north) of a magma chamber which is experiencing segregation during fractionation. The result of this would be eruption of the topmost zones of the chamber (evolved, volatile-rich magmas) in the center of the complex. The tephra explosion of 1826, originating from the central caldera, is indicative of this process.

Magma mixing, melt segregation, plagioclase accumulation and all the other mechanisms which have been previously discussed further indicate existence of a region where melts can accumulate, evolve and mix. The clinopyroxene evidence suggests crystallization occurs as deep as 10 Kbar. This roughly corresponds to a depth of 30 km. The base of the crust below Eyjafjöll is shown to be around 15 km, or about 5 Kbar pressure (RRISP 77, 1980). If melt formed below this depth, it would presumably rise (from buoyancy forces) until it reached the crust. It would remain there (at 15 km, 5 Kbar pressure) and fractionate until eruption occurs.

REE Data - Discussion

Rare earth element (REE) abundance data for the seven samples analyzed show similar trends (Figure 5.08); that is, light rare earth element (LREE) enriched, with parallel slopes. This suggests that they all melted under uniform conditions as differences in percentage of melt will change the slopes of the trends (especially at small percentages). It is interesting to note that slight positive europium anomalies exist for nearly all samples as well (Ey-4B is the only exception). One possible explanation for this is small amounts of plagioclase accumulation. Plagioclase crystallization would be expected (under the right oxidizing conditions) to preferentially extract europium (Eu^{+2}) from the melt. The amount of europium with a +2 charge is dependent upon the oxidation state (fugacity) of the system. The more reduced the

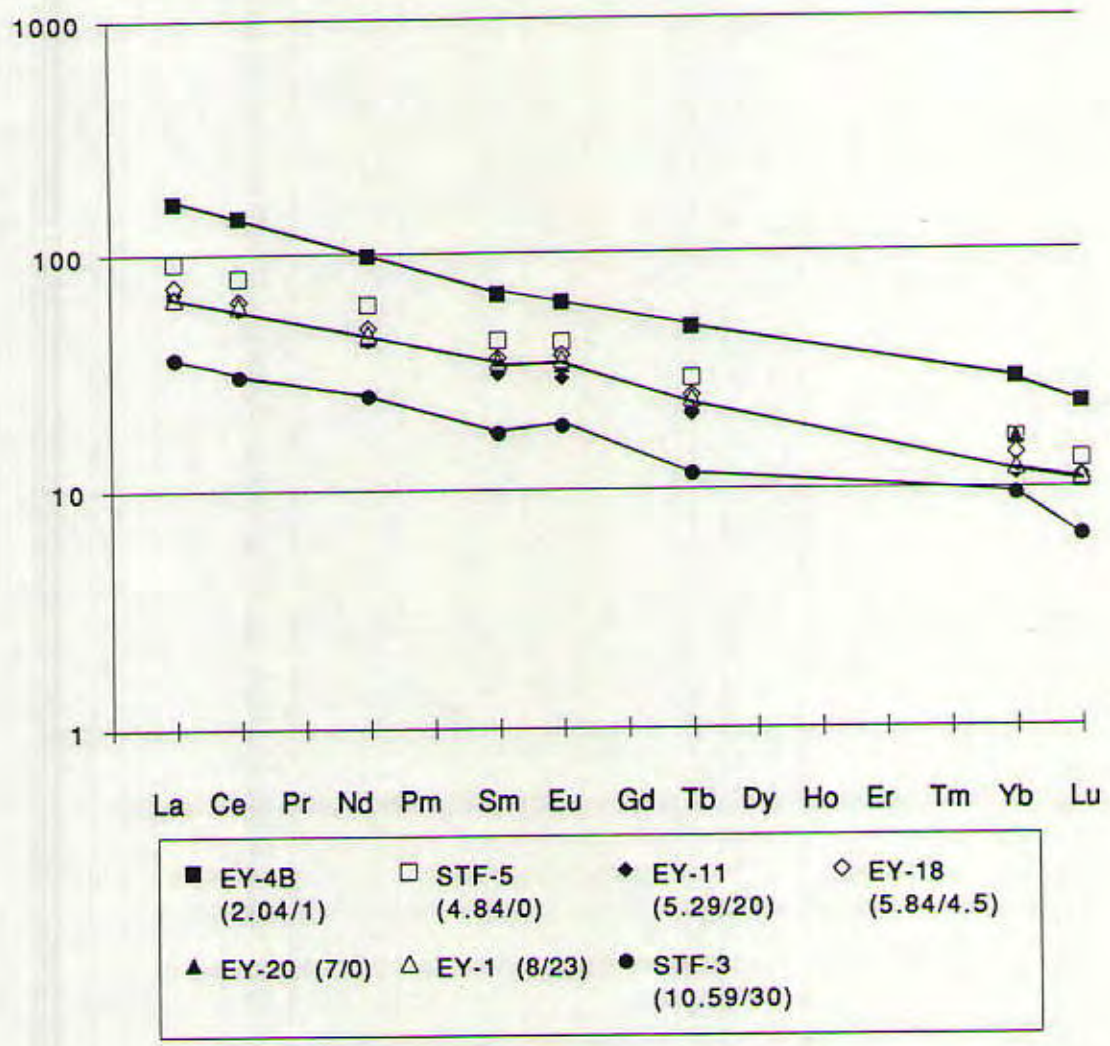

Figure 5.08: Chondrite-normalized REE patterns for Eyjafjöll samples. Numbers in parentheses refer to wt % MgO and % phenocrysts, in that order.

environment, the more Eu+2 exists and therefore the more obvious trends will be seen due to plagioclase activity. The QFM buffer is more reduced than the NNO and therefore would result in more Eu+2. For example, for alkali basalts at oxygen fugacities of QFM or above, at temperatures of 1200°C or below, Eu+2/Eu+3 of the liquid is less than 20%. This will make it much harder to see europium anomalies than if the oxygen fugacity buffer were lower (more reduced) and with higher fugacities it gets even more difficult (Drake, 1975). It appears difficult then to constrain quantitatively what these anomalies mean; they are very slight and could suggest addition of plagioclase.

If this is true then the plagioclase must be coming from other sources (and thereby bringing extra europium to the melt). STF-3, Ey-1, Ey-11, and Ey-18 all have plagioclase phenocrysts suggestive of this. However, this does not explain the slight positive anomalies seen for samples for STF-1 and Ey-20 which have no phenocrysts. Why would these samples have positive europium anomalies? It could be due to assimilation of crustal material enriched in europium from past plagioclase accumulation. This seems unlikely, however, because of the uniform slopes of the samples. Addition of partial melts of a garnet-rich amphibolite would have an effect on the REE trends, most noticeably by changing the slopes depending upon how much crust in melted and assimilated (small melts = highly LREE enriched slopes, large melts = small LREE enrichment). These differences are not seen; Eyjafjöll trends are all uniform. With a plagiclase-rich crust (typically of middle crust as descibed by Steinthórsson et al., 1985) that doesn't completely melt, a negative Eu anomaly would be expected (again not seen), because the melts would be plagioclase poor. With a kaersutitic amphibolite (lower crust as described by Steinthórsson et al., 1985) there is no garnet, so large melts of this zone would be expected to flatten out the Eyajfjöll curves. Alternatively,

and more likely, the positive Eu anomalies for material with no plagioclase phenocrysts could be a result of assimilation of plagioclase crystals (from other magmas) which melted and homogenized with the melt prior to eruption.

The differences in absolute amounts of REE abundances seen in the Eyjafjöll data can be explained by differing amounts of crystal fractionation. As the magma crystallizes, the rare earth elements will all become preferentially enriched in the liquid, so that little crystallized magmas will be lower in REE than largely crystallized magmas. This was modeled with the same MIXNFRAC program discussed earlier, at the NNO buffer, with perfect closed-system fractional crystallization, and with REE abundances similar to those from STF-3 (the lowest of the group). The results of the model agree very well with the real data according to Figure 5.08 and 5.09, where trends are shown up to 80% crystallization. The samples are listed in the legend in decreasing MgO content and consequent increasing amount of fractionation (most primitive is last), and show that the REE fractionation also agrees with the major elements.

Comparison of the REE with other trace elements (e.g., Nb and Zr) shows again that all ranges can be explained by fractional crystallization (Figure 5.10). In fact, a combination of all incompatible trace elements from these same Eyjafjöll samples (Figure 5.11) compared to normal MORB values (data from Sun and McDonough, 1986) displays consistent enrichment for the Eyjafjöll system. This is further support for a hotspot (undepleted mantle) component in the source composition for Eyjajföll volcanics.

Melting models were run using partition coefficients for the rare earth elements presented in Furman et al. (1991). Using a Rayleigh fractional melting equation and a 3 x chondrite mantle abundance, REE compositions were determined for low percentages of melt (1-6%). These compositions

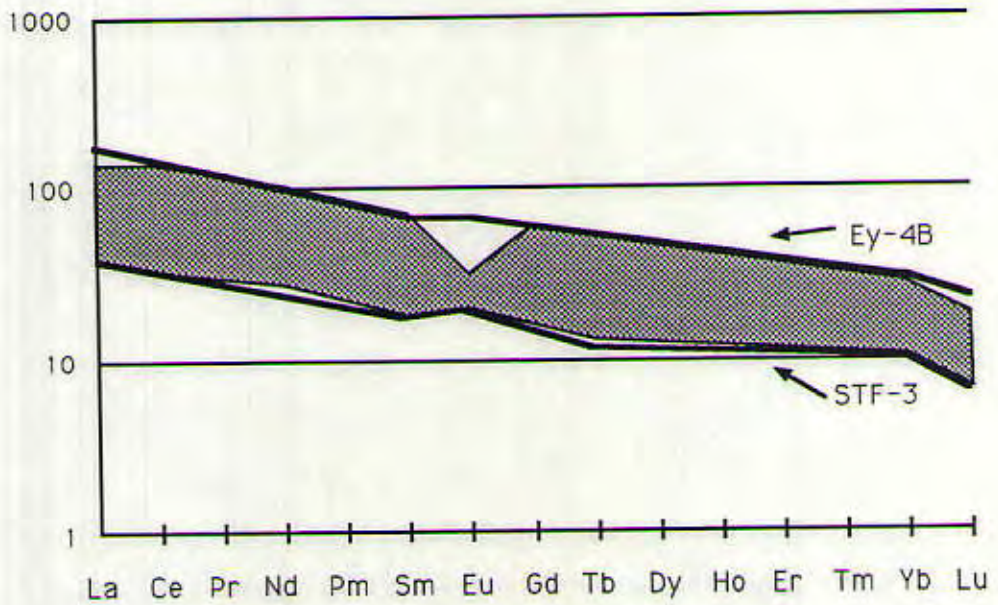

Figure 5.09: Chondrite-normalized REE patterns for Ey-4 and STF-3 (representing the highest and lowest abundances for Eyjafjöll). Background field represents range of patterns for 0-80% fractional crystallization (0-0-0 model).

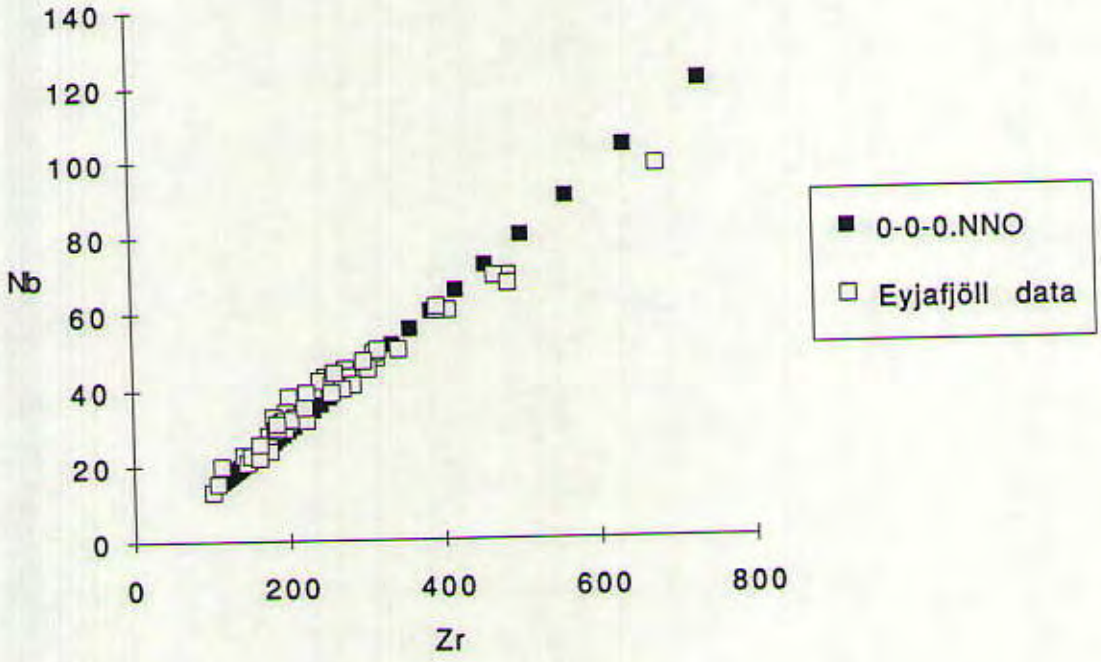

Figure 5.10: Nb and Zr variations for Eyjafjöll data combined with modeled fractional crystallization trend.

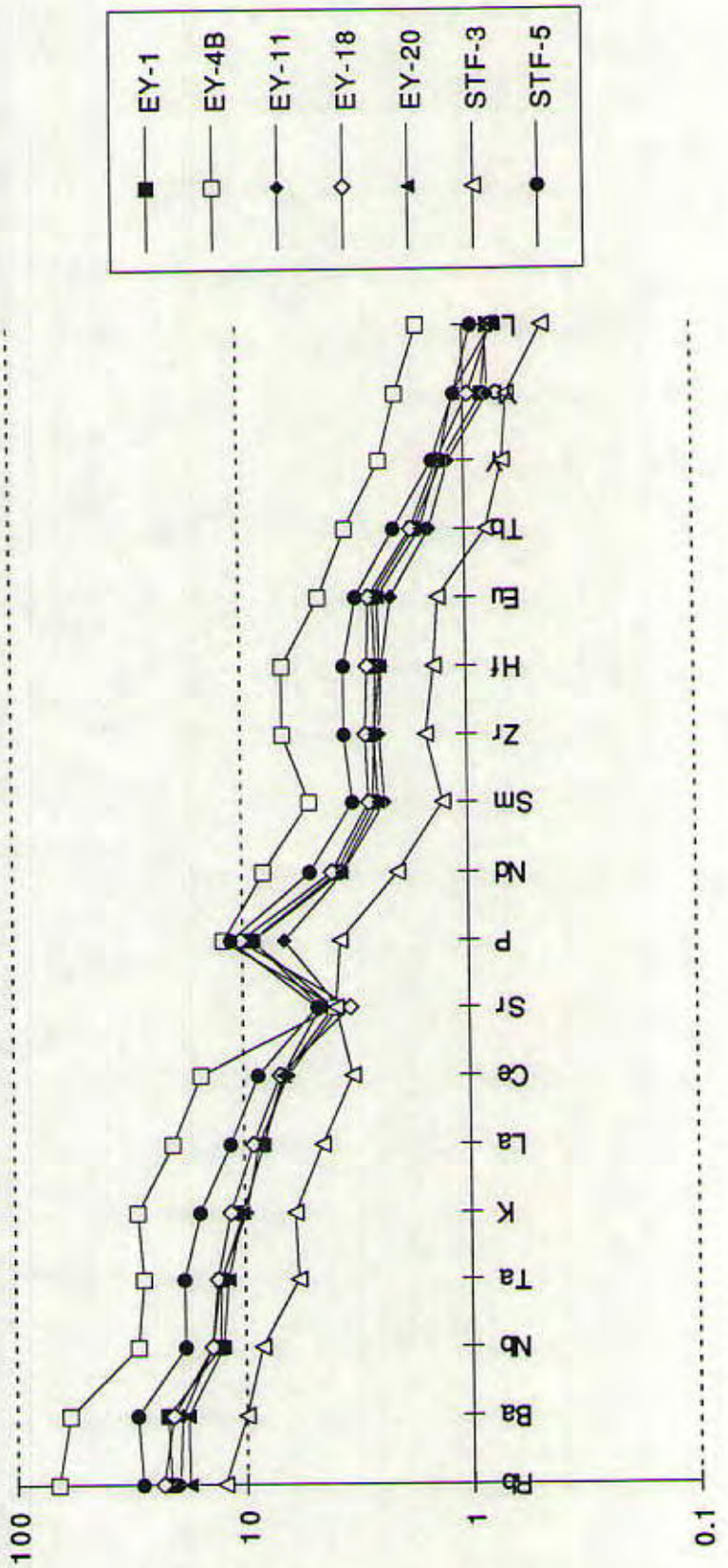

Figure 5.11: Incompatible element patterns for Eyjafjöll samples, normalized to normal MORB (NMORB) concentrations.

undergoing varying amounts of fractional crystallization are able to produce all the observed REE trends shown in Figure 5.08 and 5.09. Using Zr and Nb abundances from a similar, undepleted mantle (data from Sun and McDonough, 1986), melt models were run, and again they produced legitimate parent magma compositions for melts of 1-6%. (A legitimate parent magma is one which after small amounts of crystallization would produce the lowest trend observed in the Eyjafjöll data). It's important to recognize the limited use of these models, because precise information about partition coefficients and source composition (phases) isn't known. Similar models done for the system of Vestmannæyar to the south show melts from 1-6% from a source where garnet is < 5 volume % (Furman et al., 1991).

In order to produce a LREE enriched trend, there must be small amounts of melt from a source containing minor amounts of a phase with which HREE are compatible (perhaps garnet). Because the slopes are all parallel and the percentage of melt is quite low, the amount of garnet must be quite small. This is because any small difference in percentage of melt (1-2%) would change the slopes of the trends if the source is garnet-rich. Also, the more garnet in the source, the steeper the slopes for small amounts of melt. Eyjafjöll samples don't show slopes as steep as those associated with garnet-rich sources (comparison with REE diagrams produced from garnet lherzolite melts from Meyer et al., 1985). This seems to suggest a spinel lherzolite source for Eyjafjöll with minor amounts of garnet, and small percentages of melt.

Helium Data - Crustal Assimilation?

The REE trends (LREE enriched) are indicative of a hotspot source (as discussed in Chapter 1). High helium isotope ratios (18-19 x atmospheric) also support a more primordial source material, with values indicative of an undegassed source. There is a limitation of the use of helium values for

determination of source composition. This comes from previous work in Iceland which shows the decoupling of helium from other isotopic indicators. Whereas Sr, Pb and Nd all show significant changes when moving from Iceland to surrounding Mid-Atlantic Ridge, helium drops off much more slowly with values which are still quite high (anomalously so) along the Mid-Atlantic Ridge north and south of Iceland (Poreda et al., 1986). This has been explained by the greater effect of plume material on the helium isotope signature than MORB source material (as a result of the higher amounts of helium present in the plumes than in the depleted mantle). This is quantitatively discussed in Kurz et al. (1985) showing that even small amounts of plume material present in the source will cause plume helium signatures to dominate. For this reason it is difficult to use helium to determine proportions of plume material to MORB source material (unless helium values and contents of both endmembers can be well-constrained).

Eyjafjöll samples show remarkable uniformity in helium values, for multiple rock compositions and a large age range. Knowing the strong affect of plume material on the helium signature of the region, this probably implies that plume material has remained a steady source for Eyjafjöll, always present at a high enough proportion to dominate. In Kurz et al. (1985) it is suggested (dependent of course on helium contents of both potential sources and any possible assimilant) that 10% plume material is enough to dominate helium isotope signatures. It's possible that if conditions are right, only 1.7% would be needed. (Other isotope data would be necessary to determine more certainly what the source composition really is for Eyjafjöll).

For this same reason crustal assimilation effects will show only small changes in helium isotope ratios. For 10% assimilation (of material similar to the oldest - 16 Ma - rocks found in Iceland), the helium isotopic ratio will

change only 10% (Kurz et al., 1985). This will bring ratios starting at 20 x atmospheric to 18 x atmospheric. For the difference in Eyjafjöll samples the only assimilation possible using these maximum values would be < 10% (moving from 19.4 to 17.4 x atmospheric - the total possible range in Eyjafjöll samples). Of course more undetected assimilation can occur if the assimilant is younger crust. Though crustal assimilation cannot be completely dismissed, there is no evidence it's occuring in any great proportion. (In fact REE trends suggest that if it occurs at all it's a very small, undetectable amount, unable to change the REE trends of the rocks).

Helium isotopes alone are not enough to determine whether small amounts of crustal assimilation are occurring in the Eyjafjöll system. However, the question of crustal assimilation causing the alkalic character of Eyjafjöll has a more definitive answer. This is due to work done for other systems in the SEVZ (as discussed in detail in Chapter 2), and also from the helium work in Eyjafjöll. Comparing a tholeiitic rock, Ey-32 {19.4 x atmospheric}, with an alkalic rock, Ey-39 {19.4 x atmospheric} it can be seen that the helium ratios are exactly the same whereas if the alkalinity is due to assimilation Ey-39 should have lower helium isotope ratios. Furthermore the range for the whole system is very narrow, all within <10% differences of each other. It seems quite unlikely for assimilation to occur in the alkalic rocks and not in the tholeiites and yet lead to no difference in the helium isotopes.

An even more convincing argument against crustal assimilation as the cause of the alkalic character of this region was discussed in Chapter 2. Melting of amphibolite crust (metamorphosed basalt), with or without added water, forms trondhjemitic melts, low in K and other elements (Beard and Lofgren, 1991). This is the first experimental study of the previously only qualitative argument that crustal assimilation creates alkalic melts. Finally,

there is another, well-studied method of forming alkalic magmas which is without doubt occurring beneath the SEVZ. This is discussed further below, but it seems reasonable to conclude that crustal assimilation is not the process which is producing alkalic magmas.

Formation of Alkalic Magmas

Samples from Eyjafjöll span the whole range of compositions from tholeiitic to alkalic. An alternative method for generating this variety of compositions (as opposed to crustal assimilation) is changing in the depth and percentage of melting of mantle. Tholeiites can be formed by melting at shallow depths and relatively large degrees of partial melting while alkaline rocks form from melting of the same mantle material at greater depths and lower degrees of partial melting (Jaques and Green, 1980; Stolper, 1980). The crustal thickness attributed to the SEVZ in general and Eyjafjöll in particular, are all much greater than elsewhere in Iceland, where tholeiites are the dominant material forming. The SEVZ region consists of older crust, which has already seen a number of previous episodes of rifting and buildup, thereby thickening the crust and deepening the melt zone (Helgason et al., 1984, 1985). The implications of this anomalous depth and the present rifting in this older crust will be discussed in the last section of this chapter.

Using equations and experimental data from Langmuir et al. (1991) a modeling program was written to determine MgO, FeO, Na_2O and K_2O wt % concentrations of partial melts of mantle material. This is based on the ideas presented by Klein and Langmuir (1987) who suggested that changes in Mg and Fe can be due to changes in crustal thicknesses. With changing initial pressures (corresponding to depths and crustal thicknesses) and changing starting compositions (different source material), a series of melts are produced as fraction of melt increases, and pressure decreases. (This occurs as

the geotherm intersects and exceeds the mantle solidus). The results of this model are shown in Figure 5.12. Three different source compositions are shown, for 12 and 15 Kbar starting pressures. Tinaquillo lherzolite, and Pyrolite source compositions come from Green (1973). The spinel lherzolite composition (Salt Lake Tuff, Hawaii) comes from Kushiro et al. (1968) and is also cited and discussed in Green (1973). For each starting composition and initial pressure the melt composition will change as depicted in this figure. Each data point refers to a drop in pressure of 1 Kbar, which is approximately equal to 1% melt. Also included in this figure are points labelled Eyjafjöll which correspond to compositions of the parent magma (Ey-49) as it undergoes olivine fractionation. Any of these compositions (up to plagioclase crystallization) can represent the possible primary melts (parent magmas) for the Eyjafjöll Volcanic System.

A 3% melt of the spinel lherzolite composition at 12 Kbar, or 1% at 15 Kbar is quite similar to the composition of the most evolved of the possible parent magmas for Eyjafjöll. The more primitive parent compositions correspond to slightly higher pressures and greater degrees of partial melting but are more likely only a result of olivine addition to the magmas formed at 12 and 15 Kbar. Three compositions, the spinel lherzolite, and the most primitive and evolved of the possible parent magmas are given in Table 5.02. This model of 3% melt of a spinel lherzolite source matches well with that determined by the REE trends earlier in this chapter.

This conclusion also corresponds very well with the Meyer et al. (1985) predicted model for mantle beneath the SEVZ shown in Figure 5.13 (except that they determined garnet lherzolite as the source material). In this model Eyjafjöll overlies a region where melts are created at precisely these conditions (spinel lherzolite source and 12-15 Kbar pressure, or 36-45 km

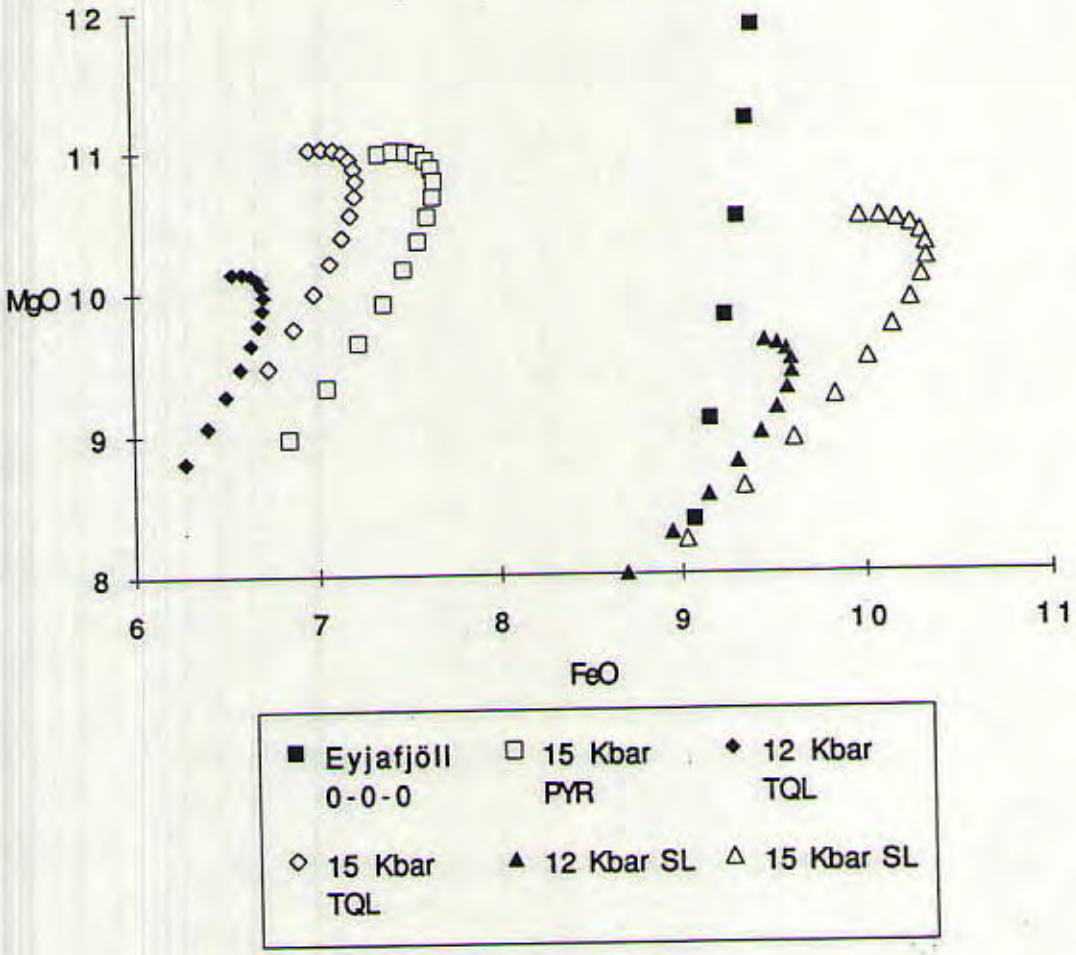

Figure 5.12: Compositions for mantle melts at different starting compositions and pressures (depths of melting). TQL = Tinaquillo Lherzolite, PYR = Pyrolite (Green, 1973), SL = Spinel Lherzolite (Kushiro et al., 1968, 1972). Starting pressures are 12 and 15 Kbar. Each data point represents a change in pressure of 1 Kbar, accompanied by approximately 1 % melt. Eyjafjöll data represent compositions of all possible parent magmas for the system. These come from the fractional crystallization models and represent all magma compositions in which only olivine is fractionating.

Table 5.02: Compositions of a spinel lherzolite (Kushiro et al., 1968), most evolved possible parent magma from MIXNFRAC fractional crystallization model (liquid just before plagioclase crystallization begins, 1187°C), and most primitive possible parent magma, from same model (Ey-49).

	Spinel Lherzolite	1187 °C	Ey-49
SiO2	48.02	47.56	46.85
TiO2	0.22	2.439	2.189
Al2O3	4.88	14.02	12.58
Fe2O3	1.94	2.731	1.76
FeO	8.15	9.069	10
MnO	0.14	0.166	0.167
MgO	32.35	8.384	12.57
CaO	2.97	12.86	11.52
Na2O	0.66	2.126	1.9
K2O	0.07	0.3136	0.28
Cr2O3	0.25		
H2O	1.11		
P2O5		0.1882	0.168
Total	100.76	99.8568	99.984

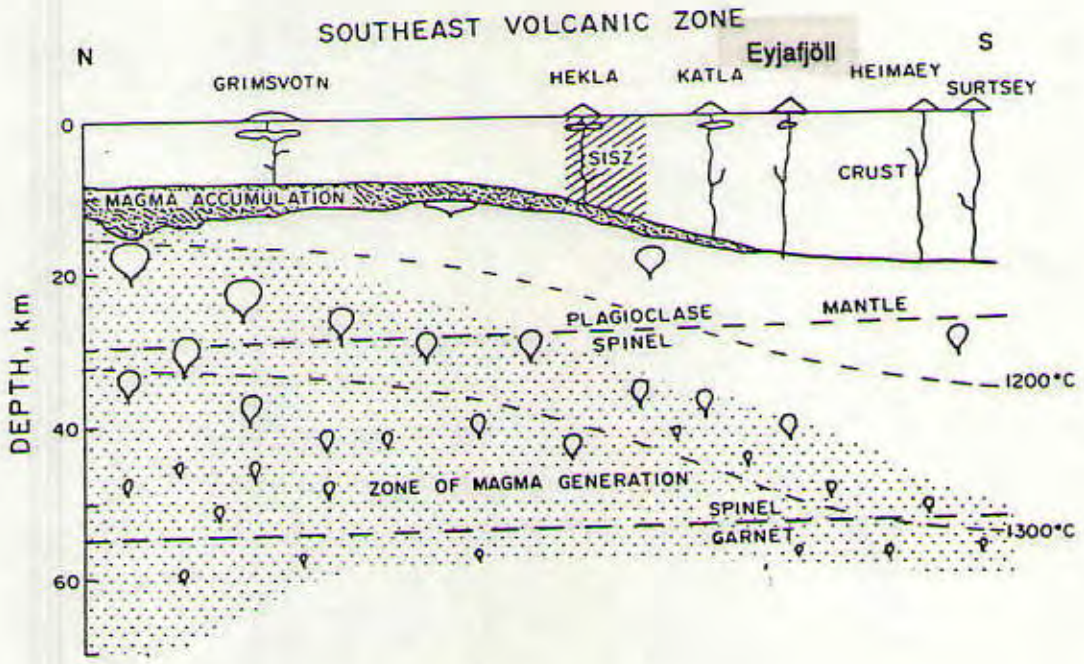

Figure 5.13: Model of magma generation and accumulation along the SEVZ. Crustal thickness is based on seismic data. The lens of magma accumulation is based on magnetotelluric data and contains 10-20% melt. Isotherms are based on geothermal gradients (from Meyer et al., 1985).

depth). Presumably this small amount of melt rises to the base of the crust where fractionation (cooling) occurs prior to eruption. Clinopyroxene data show that fractionation occurs from near surface pressures to as high as 10 Kbar (30 km). As the crust is only 15 km thick (5 Kbar), the highest pressure clinopyroxenes must be formed from fractionation during ascent of the primary melts.

As there is much support and evidence for high pressure melts forming in small percentages, and these are known from experimental work to produce alkalic magmas, this seems all that is necessary to explain the alkalic character of this region. Crustal assimilation is not necessary and in fact evidence seems to be against it as a major process.

Geochronology

Stratigraphy

The stratigraphy of Eyjafjöll, as mentioned in the last chapter, shows some age gaps, between 173 Ka and 271 Ka, and 435 Ka and 552 Ka. These gaps can be explained in a number of ways. (1) Since no sampling has been done from the northeastern or eastern edges of the volcano, the former because of inaccessibility and mapped hyaloclastites, and the latter because of the inability to differentiate between Eyjafjöll lavas and Katla lavas, it is possible that the gaps can be explained by a change in the locus of the eruptions during the missing periods toward the eastern regions of the volcano. (2) It is possible that these gaps exist due to erosion of the material by glaciers, during large transgressive events (ice ages). Evidence for four major ice ages has been found recorded in the sediments of the Tjörnes region of northern Iceland, deposited during the Brunhes magnetic period (< 0.73 Ma). These same ice ages are also found recorded in the marine sediments around Iceland, by $\partial^{18}O$ and %

$CaCO_3$ values from deep sea cores (Eiríksson and Geirsdóttir, 1991). The youngest ice age occurred at 8-12 Ka (depending upon location within Iceland). The dates of these older events are estimated at 160 Ka, 400 Ka, and 610 Ka. There is also one described as occurring just at the Brunhes-Matuyama boundary. The 160 Ka and 400 Ka ice ages could be responsible for the observed data gaps, and if so they each are required to remove a minimum of 120 Ka accumulation of volcanic material. (3) Since no sedimentary or hyaloclastite beds were sampled, it is possible the gaps can be explained as long glacial periods during which all eruptions occurred under ice, creating tephra and hyaloclastites. This seems likely, at least in part, in the Hvammsmúli and Steinafjall sections where hyaloclastites have been mapped in the regions devoid of lava flows. In particular, a large hyaloclastite region is mapped between 412 and 700 Ka in the Steinafjall section. Two large hyaloclastite beds with some intervening (unsampled) flows are mapped for the Hvammsmúli section from 350 to 600 Ka.

The existence of these beds suggests frequent changes in climate, as seven different hyaloclastite episodes are mapped within a 400 Ka time period at the Steinafjall section (Chapter 4, Figure 4.03). The effects of these climate changes are most readily seen in changes in eruptive character, when hyaloclastites dominate over flows.

Chemical Evolution of the Eyjafjöll Volcanic System Through Time

The evolution of the Eyjafjöll Volcanic System through time can be seen most clearly by the changes in composition. It appears that the oldest rocks define a very specific region within the alkalic and subalkalic zones, Figure 5.14. Figure 5.15 also shows that the oldest rocks are the most primitive (high MgO). This plot shows two ankaramites, STF-3 and Ey-49, and a

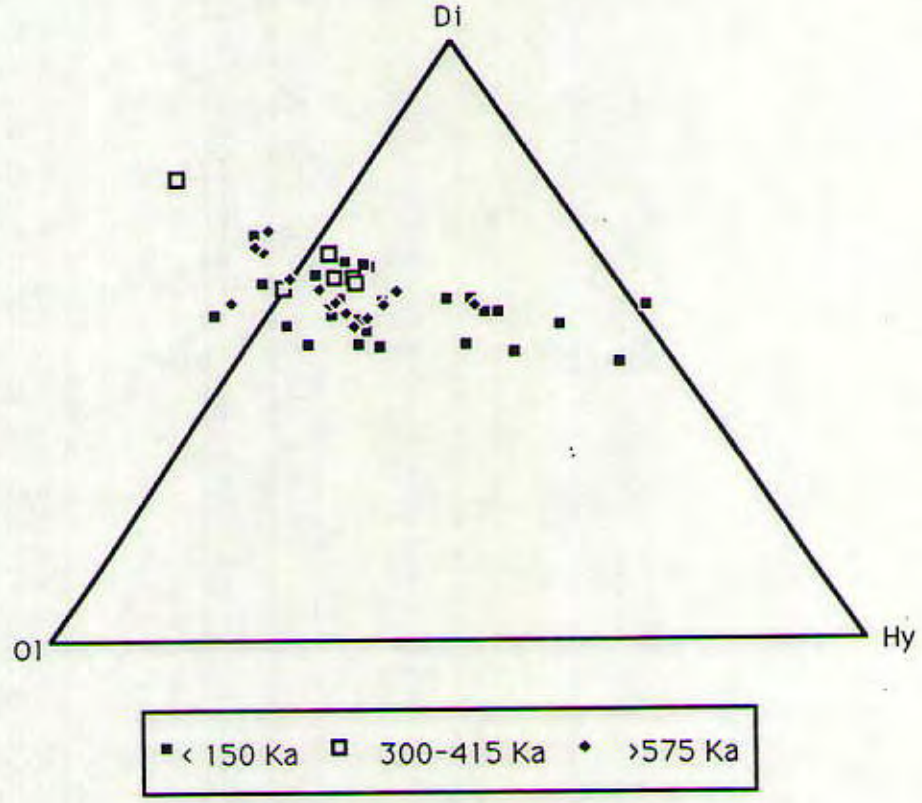

Figure 5.14: A segment of the basalt tetrahedron with Eyjafjöll data sorted according to age.

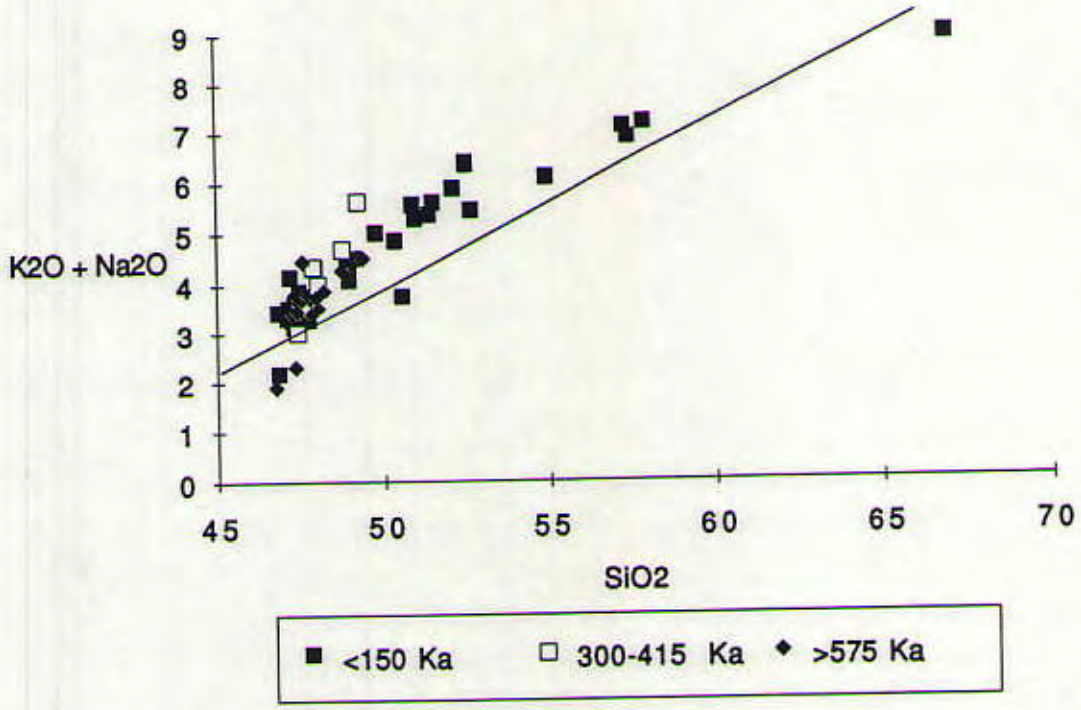

Figure 5.15: Alkali vs. silica diagram with Eyjafjöll data sorted according to age. Line indicates Macdonald and Katsura (1964) division between tholeiitic and alkaline material.

picrite, Ey-17, plotting in the tholeiite field. On the other hand, the youngest rocks of Eyjafjöll span the full range of compositions from alkalic to tholeiite, and show a much higher number of differentiated lavas. In fact, no high silica rocks are found that are older than 300 Ka. Before explaining this it is important to remember possible sampling biases. All high silica rocks found that are older than the last glacial period were found in the central regions of the volcano. If this is a trend for the system, then the older silicic rocks would be buried and unable to be sampled. However, since volcanism in the recent past has erupted basalts near the top of the system and andesites along the flanks, perhaps the sampling is representative.

There must exist some type of mechanism which can produce a greater range of magma compositions in the later periods of volcanic activity. If, for instance, the variety is due to different depths and percentage of melting (different alkali contents), then it must be explained why these were more uniform for the older lavas, and more varied in the younger ones. If melting occurred at different depths and proportions, then the parent magmas (primary melts) should be different, and consequently the trends of the oxide data should show parallel trends originating from different starting compositions. This would be particularly recognizable on the MgO vs. FeO variation diagram, as MgO and FeO will change considerably for different depths of melting. However, this is not seen, and all of the oxide variation diagrams can be explained by fractional crystallization from a single source composition and subsequent mixing among magmas with different amounts of crystallization, as mentioned earlier. It is unnecessary to invoke differing source compositions to explain this plot. In fact if multiple source compositions were present then multiple (parallel) trends would be evident from this diagram and these are not seen.

An alternative mechanism for this variety and one more likely from the point of view of the petrographic data is simply varying amounts of crystal fractionation. Greater amounts of fractionation in the near past can explain the greater variety of compositions, while in the distant past fractionation was never allowed to go very far. If this is the responsible mechanism, it is most likely due to a change in cooling rates as magmas spend more time within chambers or melt accumulation zones beneath Eyjafjöll.

If a magma chamber were able to form within the crust and allowed to fractionate over long periods of time (much like Hekla as mentioned in Chapter 2), then eruptives would be more silicic. As the only historic eruption from Eyjafjöll was a tephra explosion, a magma chamber in which a fluid phase separates and moves to the top of the chamber would be a good explanation. This would focus all silicic volcanism in the central portions of the system and make it the predominant volcanic product after long periods of quiescence. It seems, with the recent Holocene (postglacial) flows, that the silicic volcanism is increasing, perhaps indicating more time within magma chambers so that extreme fractionation can occur, whereas in the past the balance was tipped toward minimal fractionation. This explains why the oldest material on Eyjafjöll shows the least amount of fractionation, (similar to the Vestmannæyar system which also shows little if any fractionation). The implications of this will be discussed in the next section.

How the volume of material extruded at Eyjafjöll has varied through time has been estimated, as accumulation rates (Figure 5.16). These data were estimated from section thicknesses (Figure 4.03, 4.04), geological and topographical maps of the Eyjafjöll system, and K-Ar ages. The data show a fairly constant accumulation rate. The time span between 325 and 700 Ka has a lower accumulation rate and yet can be explained as a result of removal of

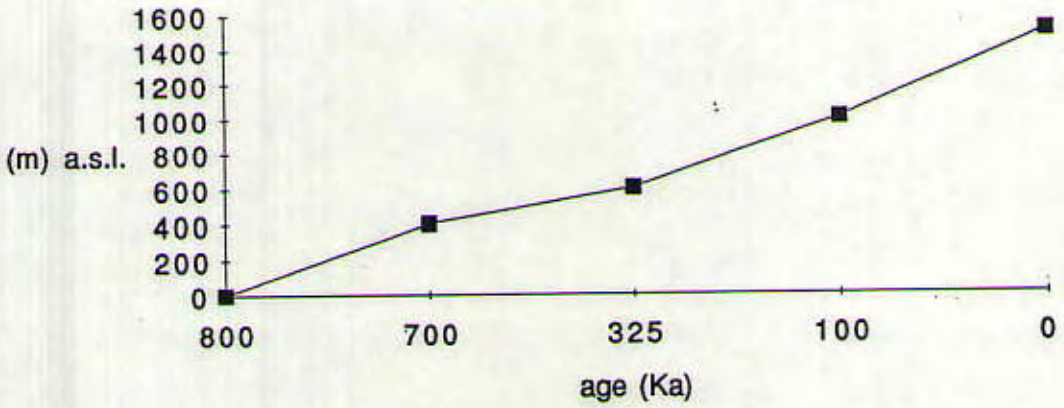

Figure 5.16: Accumulation rates for lavas on Eyjafjöll throughout known volcanic history.

material during ice ages. Eruption sites do not appear to be changing with time, in as much as the present sampling can determine. Young (<100 Ka) lavas have been erupted all over the volcano from east to west, the most recent (postglacial) along east-west fissures and in the central crater. The older lavas (>300 Ka) cropout only where glacial erosion hasn't removed them or younger lavas covered them; it is unrealistic to use these outcrops to define the extent of past volcanism.

Tectonic Implications

Trends Along the SEVZ

The volcanic system of Eyjafjöll in relation to the rest of the SEVZ was proposed in Chapter 2 to be the "missing link" to the available data. With a tholeiitic rift zone (Eastern Rift Zone) grading into a propagating rift tip (Vestmannæyar - alkalic), it would seem likely that all intermediary volcanic systems should show gradational compositions so that combined together the entire spectrum, from alkaline to tholeiitic is represented. Prior to this investigation, however, this was not the case. Vestmannæyar, the very tip of the propagator, is solely alkalic, while the Hekla-Katla regions behind the tip are solely transitional to tholeiitic. There were no data representing a gradation between the alkaline compositions and the transitional ones. Geographically, Eyjafjöll is the first system north of Vestmannæyar along strike (lying between it and the Hekla-Katla region), and thus proposed to be the best candidate to span the two different compositions. This investigation has discovered this to be true.

Two particular charts are used to demonstrate the gap and how Eyjafjöll fills it. These are shown in Figures 5.17 and 5.18. The former graph is a variation diagram of SiO_2 (wt%) vs. total alkali content (Na_2O + K_2O wt%),

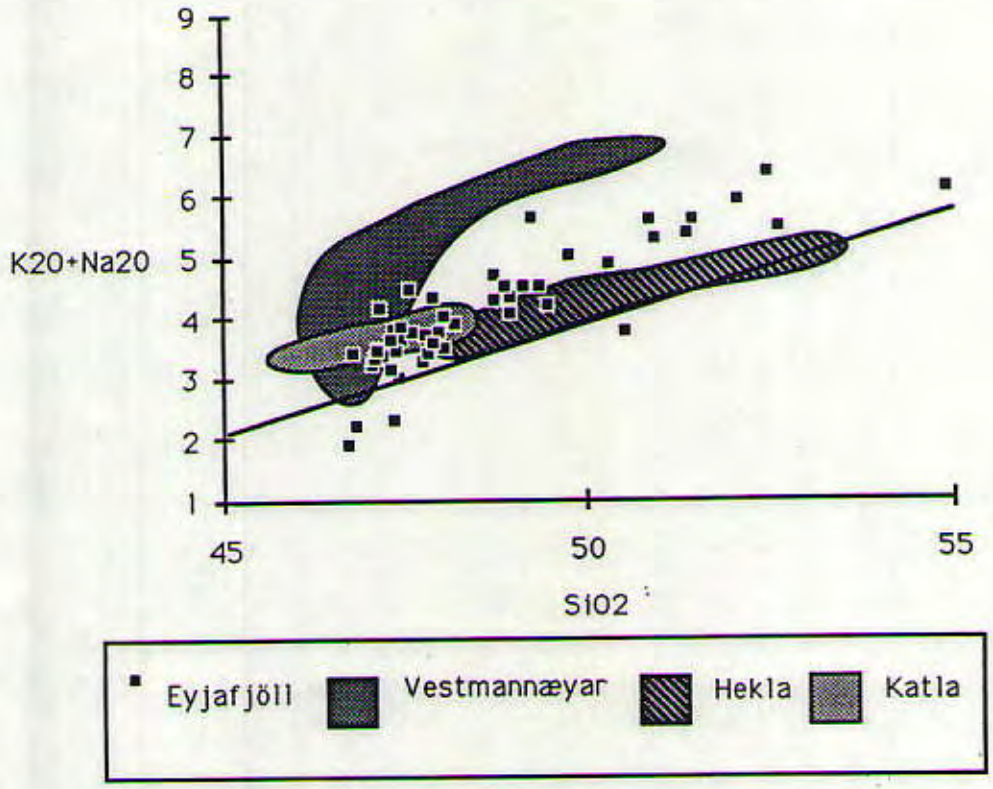

Figure 5.17: Alkali vs. silica diagram for data from Eyjafjöll, with fields corresponding to data from Hekla, Katla, and Vestmannæyar. Line indicates Macdonald and Katsura (1964) division between tholeiitic and alkaline material.

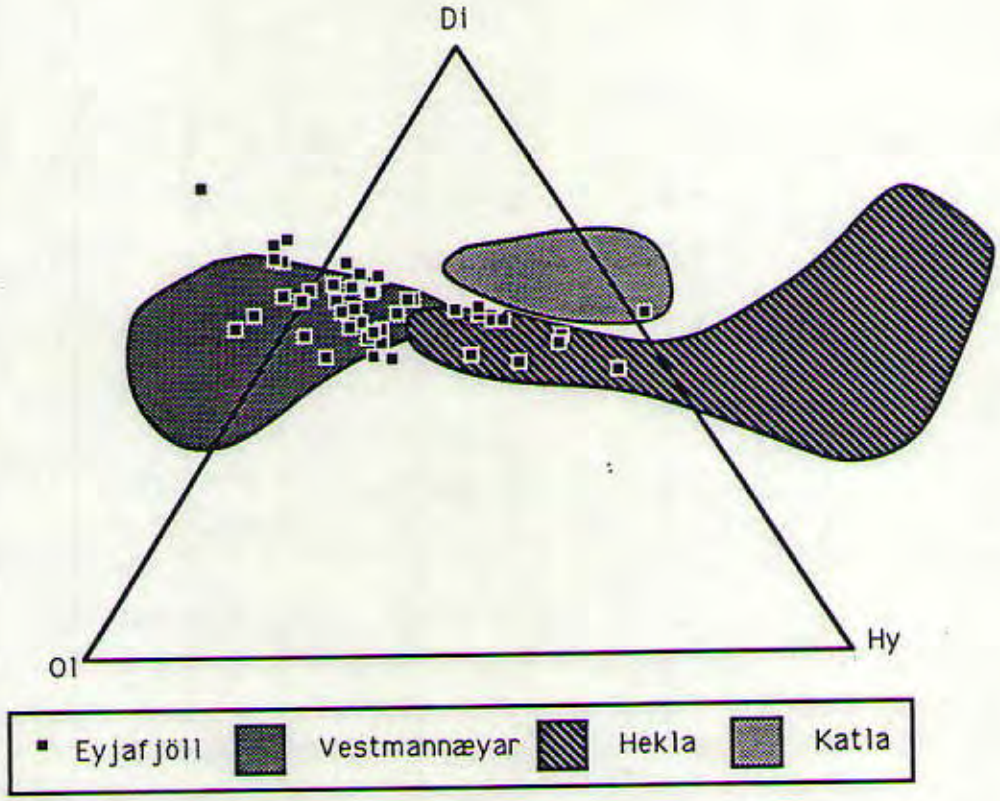

Figure 5.18: A segment of the basalt tetrahedron with data from Eyjafjöll and fields corresponding to data from Hekla, Katla, and Vestmannæyar.

similar to the one shown in Chapter 4. On this graph, the Vestmannæyar trend lies in a highly alkaline field, some distance above the Macdonald and Katsura (1964) tholeiitic-alkalic line. The Hekla system (the only system for which data on high-silica material is available in the literature) lies just above and along that same line. None of the data from these two systems overlap in this high SiO_2 range and in fact a gap does exist. In this gap, and including points which lie within both of the previously mentioned trends, lie the samples from Eyjafjöll.

Similarly, in Figure 5.18 the basalt tetrahedron is shown, and on this diagram Hekla and Katla both plot towards and around the diopside-hypersthene join, with data scattered around both sides. The Vestmannæyar data plot around the diopside-olivine join with scatter mostly on the nepheline side of this line. Between the two regions there are no data, and again no overlap. Eyjafjöll is the system which bridges this gap, with data representing the whole spectrum of compositions from nepheline-normative to quartz-normative. (It is important to note here, however, that all of the Hekla and Katla data are for recent (post-glacial) basalts and therefore represent only the latest episodes of volcanism. It is possible and likely that earlier volcanism will show similar trends to Eyjafjöll, a direct implication of this study).

The conclusion of this evaluation is that the tectonism of the region (propagating rift) and the resulting compositional variations are in fact time-progressive and geographically gradational. All grades of which <u>are</u> represented by presently active systems, and most likely in past volcanism as well. Eyjafjöll seems to have developed through magmatic-tectonic mechanisms common to both the system of the tip of the propagator and those systems further behind it. This will be discussed further below.

One other comparison among systems in the SEVZ is shown in Figure 5.19, where REE trends are shown for all systems. The slopes are consistently LREE-enriched, indicating small percentages of melt, and either surprisingly uniform melt conditions (same melt percentage everywhere) or a source which is quite low in garnet as mentioned earlier. In fact, it is predicted that SEVZ are being produced from a spinel lherzolite source. Hekla-Katla and Eyjafjöll show larger ranges for REE abundances than Vestmannæyar. This is most likely due to greater amounts of fractional crystallization in the northern systems.

Propagating Rifts and the SEVZ

Work done by Christie and Sinton (1981) addresses various characteristics seen in volcanism occurring along propagating rifts. These characteristics are compared below to the volcanism occurring along the SEVZ in the hopes of further distinguishing this region as a propagator and specifically explaining the role of Eyjafjöll. What follows is a summary of how volcanism (volumes and processes) changes relative to position along the Galapagos propagator, shown as cooling curves in Figure 5.20, and a brief explanation of to which part of the SEVZ these curves correspond.

Cooling curve A shows melting of mantle material and deep intrusions just slightly ahead of the tip of the propagator; ΔT(temperature)/Δt(time) is too high for eruptions to occur. For cooling curve B, at the very tip, isotherms have risen to the point where the first unfractionated magmas are erupted (not enough time for fractionation to occur). This corresponds to the Vestmannæyar system where mostly unfractionated magmas of small degree melts are erupting. Beyond this rift tip, heat released by cooling and crystallization of ascending magma is sufficient to cause the development of a shallow region in which temperatures exceed the basalt solidus and ephemeral bodies of magma

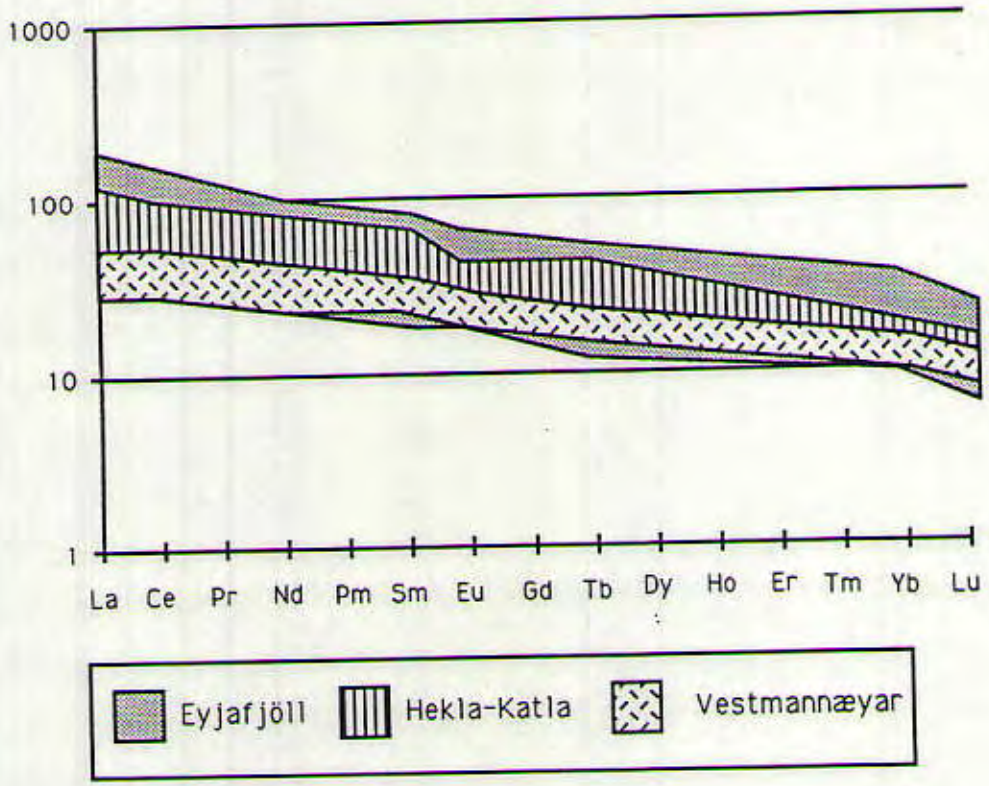

Figure 5.19: Chondrite-normalized REE patterns for samples from Eyjafjöll, the Hekla-Katla region, and Vestmannæyar.

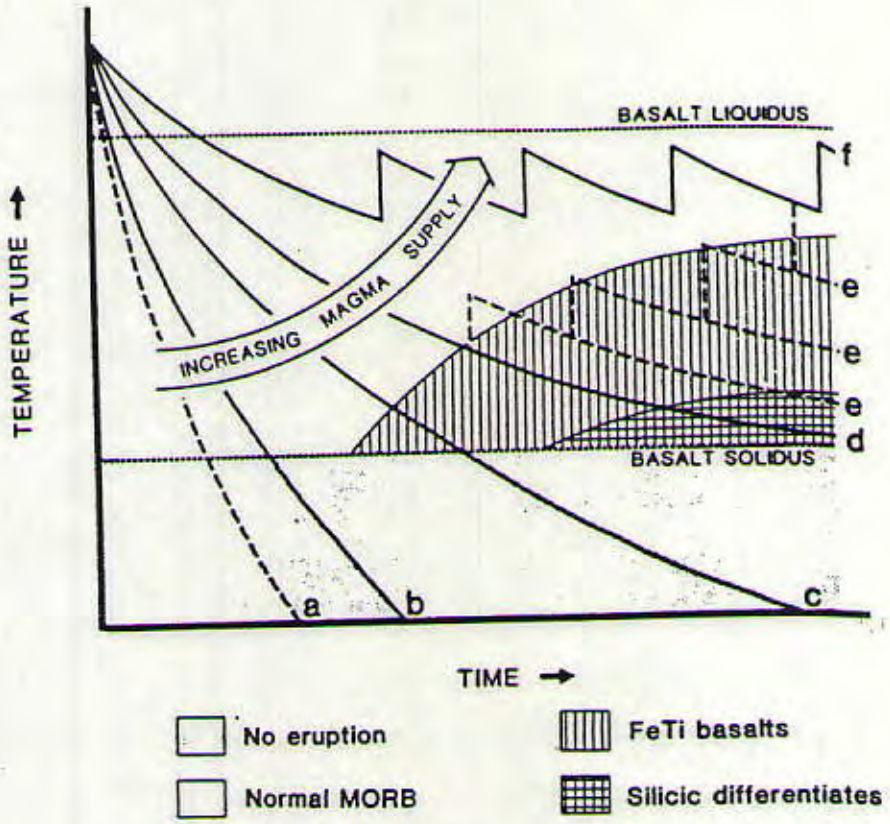

Figure 5.20: Idealized cooling paths for crustal magma bodies. Selected cooling curves are shown and discussed in text: a = cooling rate too high for eruption; b = eruption of unfractionated lavas; c = optimum for Fe-Ti basalt; d = optimum for high Si differentiates; e = increasing supply gives increased probability of mixing; f = steady state mid-ocean ridge (from Christie and Sinton, 1981).

may reside. These will undergo rapid fractionation along cooling curve C, producing Fe-Ti basalts. This curve represents what the Vestmannæyar system is presently evolving towards (Thy, 1991b), and describes the distant past of Eyjafjöll construction. The most important consequence of this diagram is that in the intermediate rates of magma supply and cooling rates, diversity of extruded lavas is maximized.

Further rise of the isotherms behind the tip causes the melt zones to enlarge. The probability of small isolated magma chambers residing and fractionating within the crust increases, cooling curve D. This curve represents the majority of Eyjafjöll volcanism, while more recent volcanism is suggestive (in part) of the curve described next. At some point behind the tip there will be a transition from ephemeral magma bodies to an increasing number of interconnected ones. At this stage, a balance is met between magma supply rate and cooling rate so that a broad range of magma compositions is formed. Compositional diversity is maintained by isolation of these magma chambers, but effects such as density separation of Fe-Ti basalts and normal basalts may become important as magma volumes and supply rates increase. Eventually interconnection of these bodies increases until a steady state system forms, curve E.

Hekla and Katla regions behind Eyjafjöll are suggestive of curve D, with a large diversity of composition and coexistence of both Fe-Ti basalts and tholeiites. Torfajökull, with its large magma chamber and extreme fractionation is most likely the region where this cooling rate vs. magma supply reaches a maximum. Further north from this system the dynamics approach steady state, curve E, and normal ridge tholeiites are erupted.

The underlying relationship governing these various curves is the balance between magma supply and cooling rate. Because the supply rate to the

SEVZ is so small there is not enough opportunity for heat to build up. As a result cooling rates are high. This is supported by the low geothermal gradients of this region as mentioned earlier in this chapter and Chapters 1 and 2. With high cooling rates, magmas will fractionate quickly. In the Hekla region cooling rates are quite fast, as described in Chapter 2; highly silicic magmas (60-65 wt % SiO_2) can fractionate in the magma chamber on the order of 50 years. Further north along the SEVZ these cooling rates with decrease as the magma supply increases.

There are some conditions present in the SEVZ zone that are different from the Galapagos propagator. These conditions end up making the distances of observed changes greater for Iceland than the Galapagos. These are listed below. (A) The presence of the South Iceland Seismic Zone will increase the cooling rate by the proximity of cool crustal material (Langmuir and Bender, 1984; Meyer et al., 1985) and as this zone is of such great length and width it will further increase cooling rates by making proximal such a large region of cool material. (B) The slow spreading rate of the Mid-Atlantic Ridge, and Eastern Rift Zone in particular will provide an even lower magma supply rate. (C) A possible lag in propagation rate of the rift relative to the underlying mantle source region will produce a corresponding lag in supply rate. Whether or not this is happening in the SEVZ is unknown. Meyer et al. (1985) suggested that it was ascension of a hotspot blob at 2-3 Ma, and lateral diffusion of this blob that instigated the propagator. If this is true, then perhaps the source is diminishing, and with it the magma supply rate. Alternatively the blob could be moving faster than the overlying lithosphere in which case magma supply is increasing. Field evidence, however, as discussed previously in this chapter suggests the former version, with a high cooling rate and low magma supply.

The Galapagos propagator shows two alkalic lavas recovered in dredge hauls (Christie and Sinton, 1981). The fact that there are fewer known alkalic rocks from the Galapagos ridge than from Iceland suggests that melting is occurring under the Galapagos propagator at lower pressures. This refers back to the work discussed in Chapter 2 by Jaques and Green (1980), where alkali olivine basalts are shown to form only in a very restricted field at high pressures and low percentages of melting. Perhaps because the Galapagos propagator overlies thinner crust than the SEVZ, 10 km for the Galapagos (Hey et al., 1986, 1980) and 10-30 km for the SEVZ, this signifies a lower depth and pressure of melting for the former. Certainly the lava compositions suggest as much.

Compositional trends in Eyjafjöll data show that the balance of magma supply and cooling rate has changed over time, most likely due to movement of the propagator to the south. Eyjafjöll has moved from a past balance similar to the present situation in Vestmannæyar, to a balance today which appears to be approaching the balance of Hekla. Possible rates for this propagation can be determined only in approximate terms. The best method for determination would be by comparison among all the systems of the SEVZ of changes in cooling rates. Unfortunately none of the other systems have been extensively studied into their past. As discussed in Chapter 2, drill cores of the Vestmannæyar System show emergence of the alkalic present day character (180 m thick section) overriding 560 m of marine sediments. Undoubtedly this transition marks the movement of the propagator forward. If the rocks found just above this change could be dated then rates could be approximated. The Eyjafjöll system, for which 780 Ka of data are available, has the most comprehensive time-composition data set. In order to approximate rates of propagation, it is estimated that Eyjafjöll was the tip of the propagator at 750 Ka. Over 600 Ka

± 100 Ka (up to the change in cooling rates at about 150 Ka ± 100 Ka) the propagator tip has migrated forward 50 km ± 10 km (distance between the center of the Eyjafjöll Volcanic system and the center of the Vestmannæyar Volcanic System). This sets the propagation rate very roughly at 0.83 cm/yr ± 0.22 cm/yr. The Galapagos propagator, in comparison, has been estimated to move at a velocity of 5 cm/yr (Hey et al., 1986); one reason it is faster than the SEVZ is probably due to the different thicknesses of crust through which they are propagating .

Tectonic Models for the SEVZ

Models for the entire SEVZ region have been previously proposed (Thy, 1991b; Meyer et al., 1985), and one in particular was discussed at length in Chapter 2 and earlier in this chapter (Figure 5.13, Meyer et al., 1985). This model seems to hold well for Eyjafjöll, and shows in cross-section how various aspects of volcanism and structure change. The most striking changes seen along the SEVZ are changes in crustal thickness (thinner away from the tip) and a corresponding change in composition (alkalic at the tip, tholeiitic along the rift). Melting of the source region for Vestmannæyar rocks has been estimated at 15 Kbar (45 to 60 km depth). In Eyjafjöll (this investigation), melts are estimated to form at 12 to 15 Kbar (36 to 45 km depth). These melts migrate upwards through the upper mantle and crust and create magma chambers at 15 km depth which corresponds to about 3 Kbar pressure. Hekla, behind Eyjafjöll shows formation of magma chambers at 10 km depth, 1 to 3 Kbar. It also shows extensive magma mixing, indicative of large interconnecting magma chambers forming melt accumulation zones. (Though no evidence was accumulated from this study, it seems likely that water content also changes, increasing further from the tip of the propagator).

As the crustal thickness changes, so too does the composition of the extrusive material. Where material melts at the highest pressures (deepest) and partial melts are the lowest (magma supply is the lowest) parent magmas are highest in alkali content and are silica-undersaturated. The volumes are quite small (percentage of partial melting) and therefore the incompatible elements are enriched. As depth decreases and magma supply increases the alkalinity will decrease. Variation in alkalinity at Eyjafjöll suggests that in the past (>500 Ka), Eyjafjöll was probably near the tip of the propagator. Today it has been replaced by Vestmannæyar but still shows gradations away from its earlier history. It has now managed to form magma chambers where highly silicic material has a chance to form, and cumulate crystal zones are created.